CHAPTER V

RESULTS AND DISCUSSION

The main topic of this research involves an attempt to clarify the reaction mechanism for the selective catalytic reduction of NO by hydrocarbon in a large excess of oxygen over Pt-based catalyst. To accommodate for the consideration in detail, the results and discussion are categorized into five sections. In the first section, the preliminary experiment to study the possibility of the formation of carbonaceous species on a Pt/Al_2O_3 catalyst under a large excess of oxygen is carried out. The characterization of a monometallic Pt/Al_2O_3 catalyst is pronounced in section 5.2. The investigation about the catalytic activity behavior and the characteristic of surface species produced on the catalyst surface in the selective catalytic reduction of NO by C_3H_6 is mentioned in section 5.3. In addition, the obtained information in this section is carefully interpreted to speculate the possible reaction mechanism. Subsequently, section 5.4 is devoted to confirm the reaction mechanism proposed in section 5.3. The technique used in this section is the addition of the second metal on a monometallic Pt/Al_2O_3 catalyst in order to disturb the function of active sites in such reaction. Finally, the methods in sections 5.3 and 5.4 are applied to use for another reductant. Hence, the mechanistic studies in the selective catalytic reduction of NO under lean-burn condition on Pt based catalysts using C_3H_8 as a reductant instead of C_3H_6 are conducted in section 5.5.

5.1 Preliminary Studies about the Formation of Carbonaceous Species on a Pt/Al_2O_3 Catalyst under a Large Excess of Oxygen

Prior to investigate the reaction mechanism of the selective catalytic reduction of NO by hydrocarbon over Pt/Al_2O_3 catalyst under lean-burn condition through the investigation of surface species on the catalyst surface, it is necessary to confirm that an apparent image of carbonaceous surface species can be obvious enough for consideration in detail because these species may possibly be lost all by the oxidation with oxygen. In general, it is well known that the temperature programmed oxidation technique has extensively been accepted in the worldwide to use for the characterization of coke deposition [206], which is an important deactivation mode in hydrocarbon conversion processes under reducing atmosphere, e.g., dehydrogenation [207], cracking [208], reforming [209] and etc. Hence, the comparative study of the formation of carbon containing species in the reactions with and without oxygen is carried out.

In this section, the 0.3% Pt/Al_2O_3 catalyst was used to study the formation of carbonaceous species in the two reactions under reducing condition, i.e., dehydrogenation and non selective catalytic reduction of NO, and in the two reactions under oxidizing condition, i.e., hydrocarbon combustion and selective catalytic reduction of NO under excess oxygen. Prior to the reaction test, 0.5 g of catalyst was reduced with a flow of H_2 at 500°C for 1 h and then cooled down from 500°C to a given reaction temperature, 350°C or 170°C in the reaction with the absence and presence of oxygen, respectively. A feed gas mixture was introduced at the volumetric flow rate of 50 ml/min or with GHSV of 4000 h^{-1}. Either propane or propene was used as the hydrocarbon reactant and their compositions were independently fixed at 3000 ppm, while the others were set on 1000 ppm NO, 2.5% oxygen and He balance being dependent on each reaction. The time on stream of all reactions was fixed at 2 h. The spent catalyst from each reaction was characterized by temperature programmed oxidation technique performed by burning it in 1% oxygen in helium.

The effect of time on stream on all reactions over 0.3% Pt/Al_2O_3 catalyst at 350°C for the reaction without oxygen and at 170°C for the reactions with oxygen is shown in Figures 5.1 and 5.2, respectively. In all reactions, it is observed that the reactions with propene as a reactant give more hydrocarbon conversion in the initial interval of time on stream than those with propane. However, in the dehydrogenation and the non-selective reduction of NO, the conversion of propene is dropped more rapidly than that of propane. When the time on stream approaches to 2 h, the reaction with propene gives less hydrocarbon conversion than that with propane.

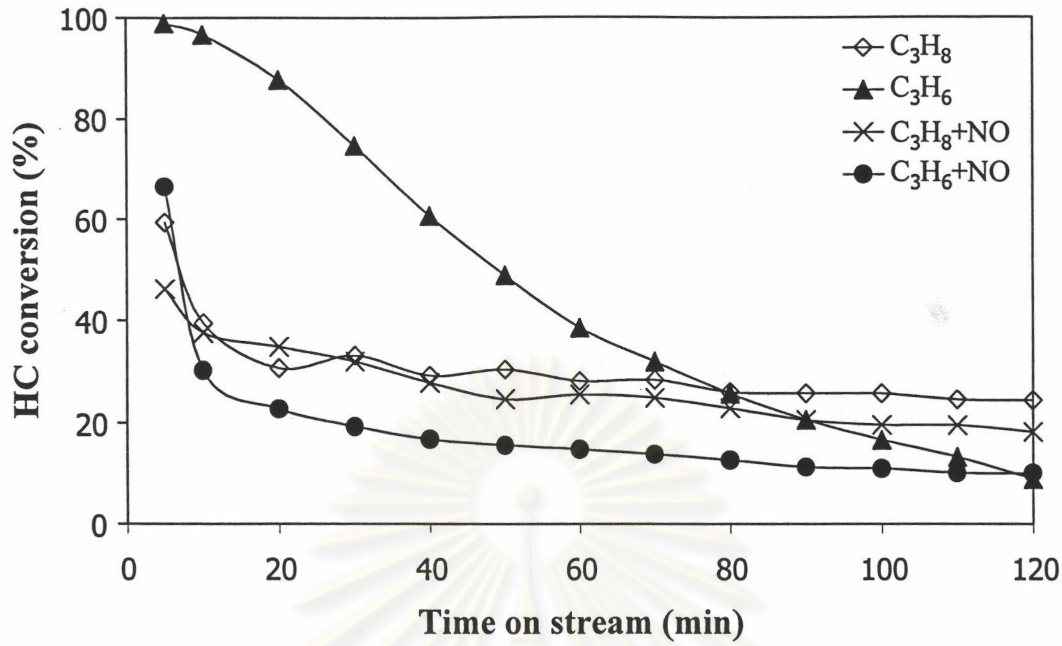

Figure 5.1 Relationship between % HC conversion and time on stream in various reactions without oxygen on Pt/Al_2O_3 catalyst at 350°C

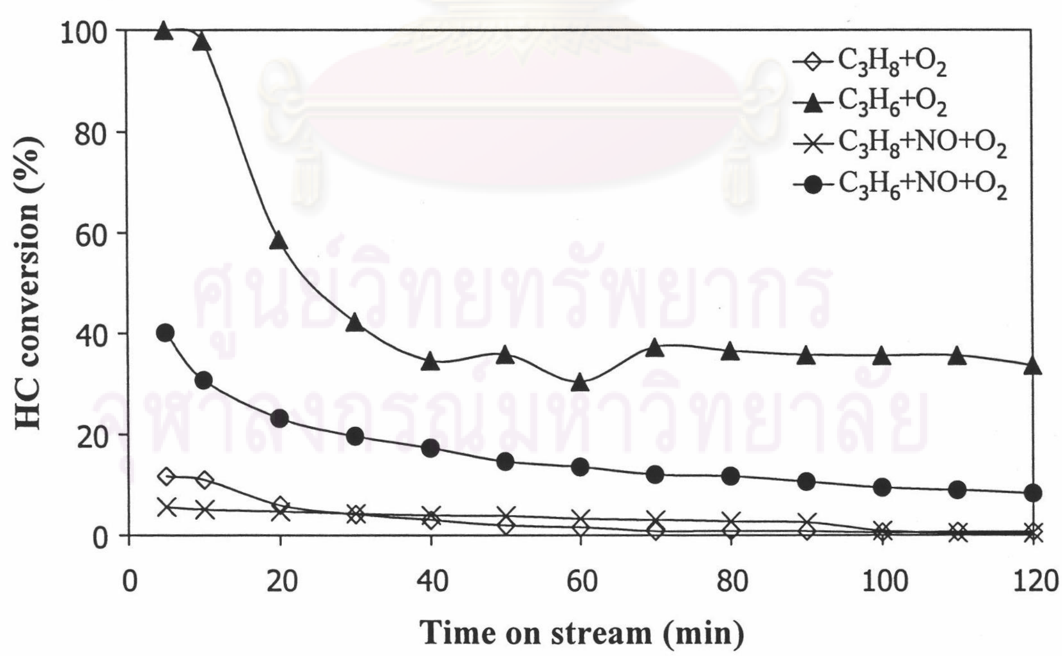

Figure 5.2 Relationship between % HC conversion and time on stream in various reactions with oxygen on Pt/Al_2O_3 catalyst at 170°C

After each reaction, 0.3 g of the spent catalyst was characterized by temperature programmed oxidation technique. The TPO profiles of the spent Pt/Al_2O_3 catalysts are exhibited in Figures 5.3 and 5.4 for the reactions without and with oxygen, respectively. Each sample obtained from the reaction without oxygen shows a TPO peak around 425°C represented to the coke on the support as reported in the previous work [210]. Considering the TPO profiles of the spent catalyst from the reaction with oxygen, the absence of NO in the feed stream results in the TPO profiles indicating a shoulder at 250°C and a TPO peak around 425°C. While the TPO profiles of the spent catalyst treated in $HC+NO+O_2$ systems shows only TPO peak at the temperature around 325°C for the reaction with propane and two peaks at the temperature around 325°C and 425°C for the reaction with propene. The percentage of carbon in the spent catalyst and the selectivity of coke formation defined as the ratio of carbon atom in carbonaceous species to carbon atom obtained from the converted hydrocarbon in feed are also calculated as shown in Table 5.1.

Table 5.1 The hydrocarbon conversion, the amount of carbonaceous species and the selectivity of coke formation for 0.3% Pt/Al_2O_3 catalyst

Reaction	Reactant	Temperature (°C)	HC conversion at 5 min (%)	Carbon in carbonaceous species (%)	Selectivity of coke formation (%)
HC	C_3H_8	350	59.4	0.17	0.22
	C_3H_6	350	98.9	0.32	0.27
HC+NO	C_3H_8	350	46.2	0.13	0.19
	C_3H_6	350	66.1	0.16	0.34
$HC+O_2$	C_3H_8	170	11.7	0.13	1.13
	C_3H_6	170	100.0	0.48	0.29
$HC+NO+O_2$	C_3H_8	170	5.6	0.12	1.07
	C_3H_6	170	40.1	0.33	0.54

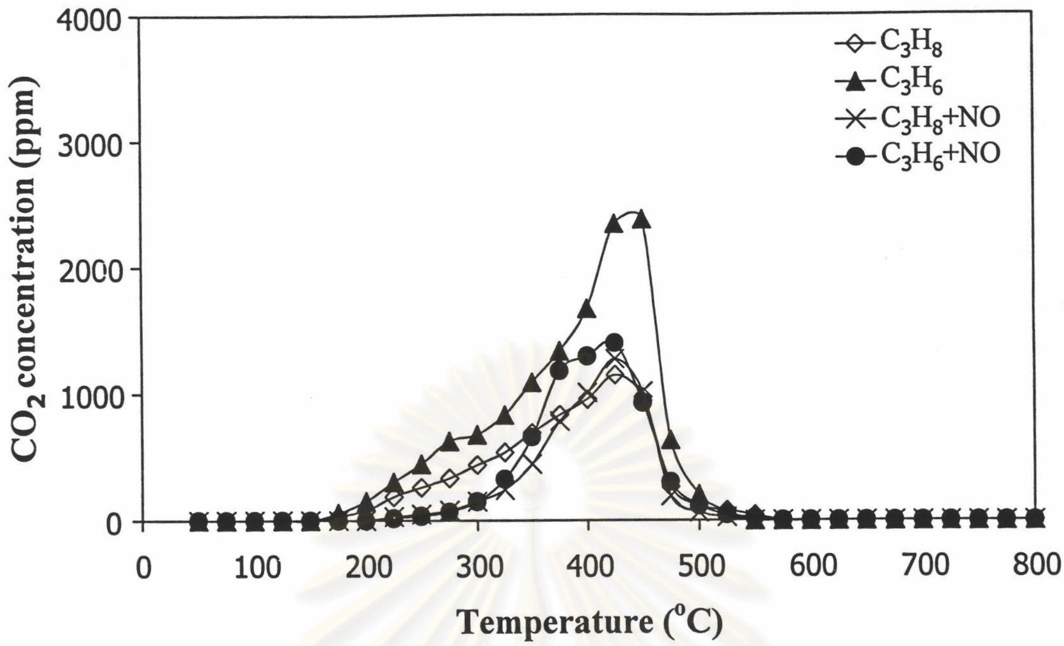

Figure 5.3 The temperature programmed oxidation profiles of the spent Pt/Al_2O_3 catalysts from various reactions without oxygen

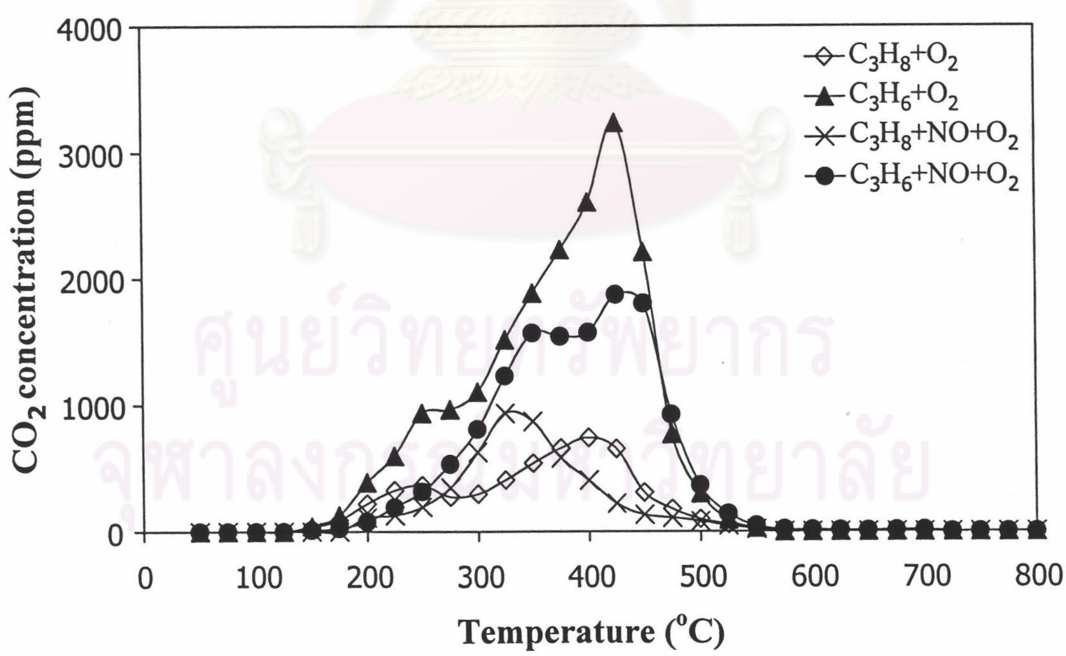

Figure 5.4 The temperature programmed oxidation profiles of the spent Pt/Al_2O_3 catalysts from various reactions with oxygen

From table 5.1, it is found that under reducing atmosphere propene gives higher selectivity of coke formation than propane, whereas under oxidizing atmosphere the results are contradictory. For the reactions without oxygen, propane is eliminated hydrogen to produce propene. The hydrogen can suppress coke formation. On the other hand, using propene as the reactant, propene can easily be added hydrogen to produce propane at this temperature. The hydrogen may rapidly be used for the formation of propane product or slightly suppress coke formation, since the selectivity of coke formation with propene is more than that with propane. It is significantly observed that if NO is introduced in the feed stream without oxygen, the amount of coke will decrease both in event of propane and propene as the reactant. When propene is used as the reactant, the presence of NO results in the decrease of a main product, propene. On the other hand, using propene as the reactant, the main product, propane, is not found in case that NO is added. Therefore, it is speculated that in the reactions without oxygen the series model of coke formation is proposed.

Under oxidizing atmosphere, it is suggested that carbonaceous species are formed in parallel with the formation of carbon dioxide. Besides, in the reaction with oxygen using propane as reactant, it is observed that the absence of NO gives a little higher selectivity of coke formation than the presence of NO. On the other hand, in case of propene, the selectivity of coke formation in the presence of NO is about two times higher than that in the absence of NO. It is possible that propane or propene is first reacted with adsorbed oxygen to be converted to the intermediate surface species. With propane, these intermediate surface species are expected to be hardly reacted with NO resulting in the equivalent of the amount of carbonaceous species and the selectivity of coke formation in the reaction with and without NO. However, in case of propene, the possible mechanism can be classified into the following two suggestions.

1. NO is hardly reacted with the intermediate surface species but it prefers to dissociate into dinitrogen. Thus, since the dissociation of NO hinders the formation of carbon dioxide, the intermediate surface species prefers to produce the remaining carbonaceous species rather than carbon dioxide in the reaction with NO.

2. Both NO and propene would compete to adsorb on the active sites. NO reacted with oxygen to produce NO_2, which could preferably reacted with propene or propene-derived species. Inasmuch as the first step is irritated by NO, it is noticed that the propene conversion and the amount of coke decrease in the reaction with NO. The selectivity of coke formation is dependent on the competition of NO and propene to react with oxygen.

Further studies are necessary to elucidate the actual mechanism of Pt/Al_2O_3 catalyst in all four reactions. However, with the above information in this section it is confirm that the formation of carbonaceous surface species is much enough for consideration in mechanistic studies.

5.2 Characterization of a Monometallic Pt/Al_2O_3 Catalyst

5.2.1 The Specific Surface Area and the Metal Active Sites

The BET surface area and the amount of metal active sites of a Pt/Al_2O_3 catalyst are shown in Table 5.2. It can be observed that a pure alumina support gives a more BET surface area than the alumina supported platinum catalyst. This indicates the plugging of the loaded platinum on the alumina pore. The platinum dispersion calculated as shown in Appendix C exhibits that the platinum atom can be rather thoroughly distributed on an alumina support when chloroplatinic acid hexahydrate is used as the platinum precursor.

Table 5.2 The platinum composition, the specific surface area, the metal active sites and the platinum dispersion on a Pt/Al_2O_3 catalyst

Sample	Pt content (%wt)	The single point BET surface area (m^2/g sample)	Metal active sites ($\times 10^{19}$ molecule of CO/g sample)	Pt dispersion (%)
Al_2O_3	-	285	-	-
Pt/Al_2O_3	1.0	269	2.55	83

5.2.2 X-ray Diffraction Pattern

X-ray Diffraction is an important technique identifying the crystal structure. The XRD patterns of a pure alumina support and the fresh 1 wt% Pt/Al_2O_3 catalyst are illustrated in Figure 5.5. It can not be observed the difference between both XRD spectra. This means that the amount of platinum on the catalyst surface may be not enough to be detected by this technique or the platinum particle size may be quite small. It is remarked that both XRD spectra definitely show the characteristic peak of amorphous γ-Al_2O_3 [211].

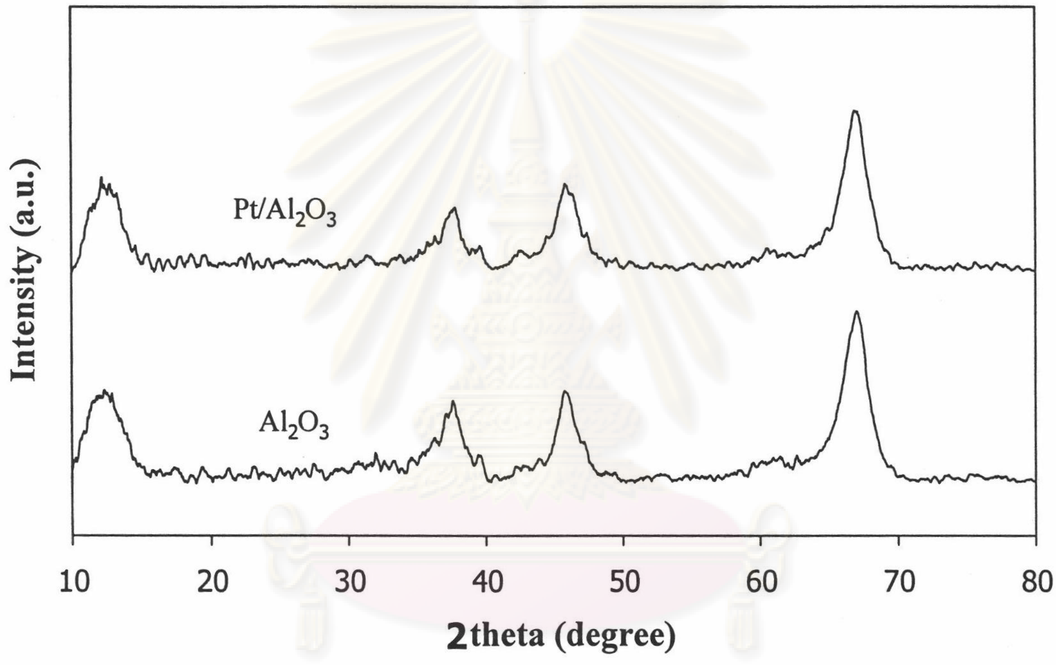

Figure 5.5 X-ray diffraction pattern of a pure Al_2O_3 support and a Pt/Al_2O_3 catalyst

5.2.3 Acidity Behavior

In general, strong bases, as adsorbates, should in principle be suitable probes for the evaluation of the overall acidity of catalysts, as well as to distinguish between protonic (Brønsted) acidity and aprotic (Lewis) acidity. In this work, pyridine and ammonia are independently used as probe molecules for acidity measurements. It is remarked that the different familiars of acid sites are characterized by pyridine adsorption technique whereas the total concentration of acid centers at the catalyst surface is measured by ammonia temperature programmed desorption (NH_3 TPD) method.

Figure 5.6 demonstrates the infrared (IR) spectra obtained from the adsorption of pyridine on 1 wt% Pt/Al_2O_3 at room temperature followed by the temperature programmed desorption under vacuum up to 500°C. It is observed that the spectrum of the adsorbed pyridine at room temperature shows the obvious band at 1445 cm^{-1} due to adsorbed pyridine on Lewis acid sites as previously reported in other published work [212]. On the other hand, the bands at 1545 cm^{-1} and 1635 cm^{-1} representative to pyridinium ion on Brønsted acid sites can not be detected on this catalyst. The 1640-1550 cm^{-1} spectral region involving the bands at 1578 cm^{-1}, 1593 cm^{-1} and 1614 cm^{-1} is likely assigned to be adsorbed pyridine on Lewis acid sites [213]. The two formers are formed whenever Al ions possess the sole octahedral coordination while a prevalent latter indicates the presence of the tetrahedral coordination of Al ions [213]. It is noted that only the 1491 cm^{-1} band can not be addressed to a single site. This result suggests that on Pt/Al_2O_3 catalyst only Lewis acid sites are present. After heating under evacuation from room temperature to 500°C, it can be seen that all bands gradually decrease with increasing temperature until hardly detectable at 500°C.

To study the acid strength of Lewis acid sites, the rate of desorption as well as the amount of desorbed pyridine on Lewis acid sites at various temperatures are closely observed by focusing on the distinct band at 1445 cm^{-1} as shown in Figures 5.7 and 5.8, respectively. It is found that most of adsorbed pyridine on Lewis acid sites are dramatically released at temperature below 200°C. Nevertheless, there are about 10% of the adsorbed pyridine remaining on the catalyst surface at temperature above 300°C. This indicates that a majority of acid sites on Pt/Al_2O_3 catalyst behaves the weak Lewis acid sites.

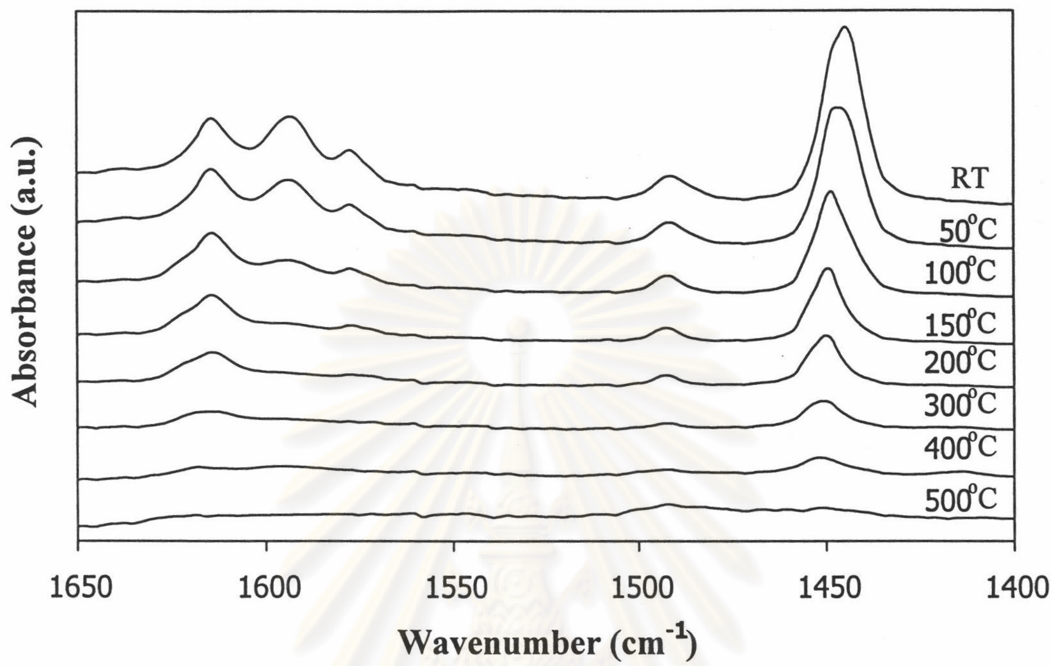

Figure 5.6 IR spectra after pyridine adsorption on Pt/Al_2O_3 catalyst at room temperature followed by heating under evacuation at various temperatures

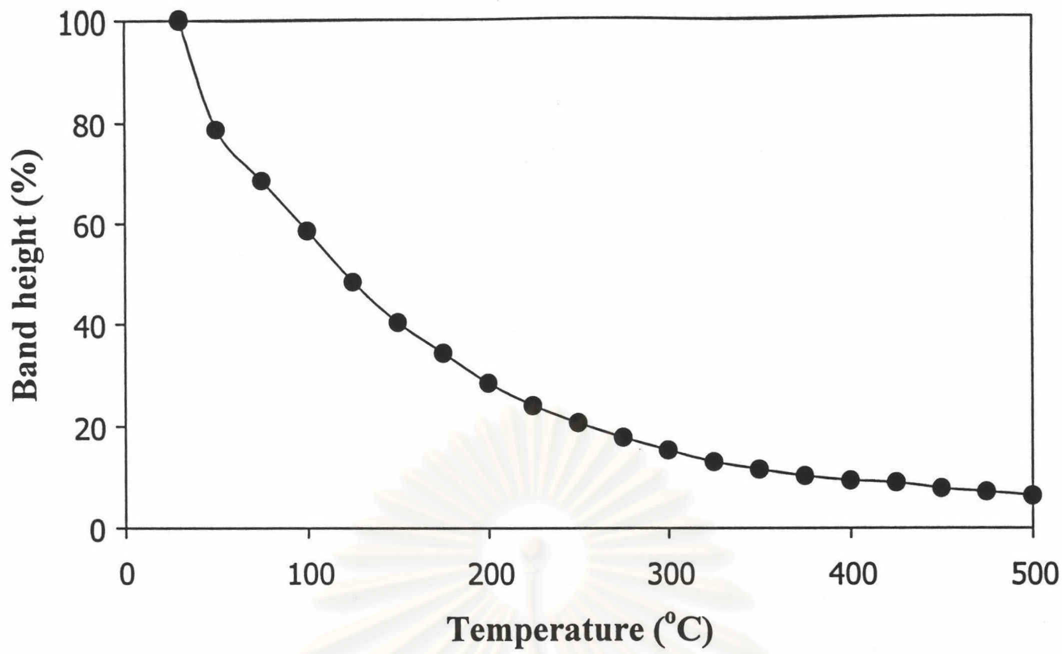

Figure 5.7 The percentage of adsorbed pyridine remaining on Lewis acid sites of Pt/Al_2O_3 at various temperatures by focusing on the band at 1445 cm^{-1}

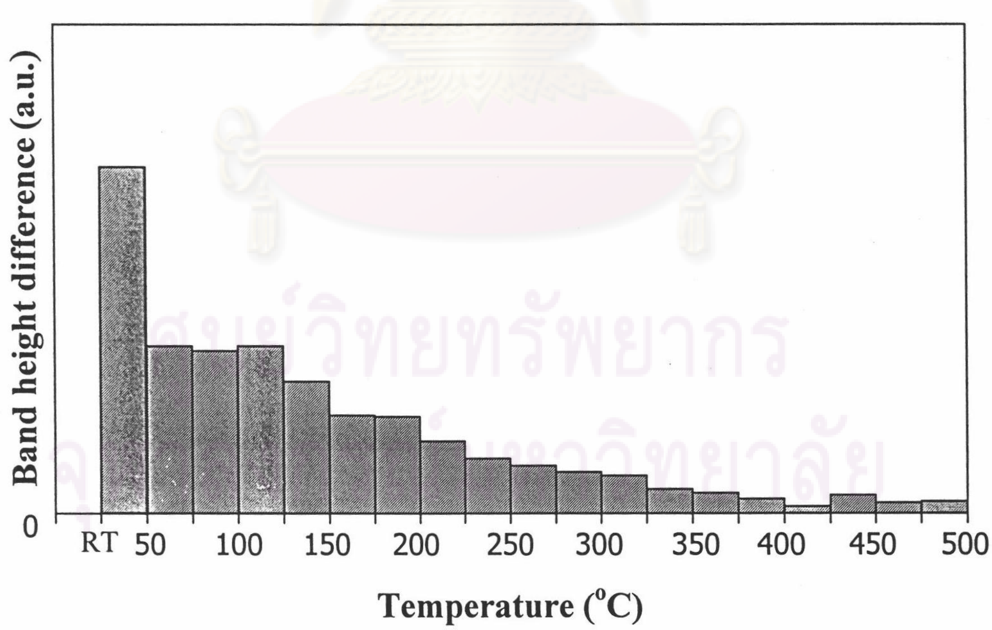

Figure 5.8 The amount of desorbed pyridine releasing from Lewis acid sites of Pt/Al_2O_3 at various temperatures by focusing on the band at 1445 cm^{-1}

In order to provide more complete information about the characteristics of the surface acid sites of a Pt/Al_2O_3 catalyst, the acidity measurement was also carried out by the conventional temperature programmed desorption of ammonia. Although this procedure can not resolve to discriminate between different types of acid sites, it is routinely used to evaluate the total acidity of catalysts. The spectrum obtained with 1 %wt Pt/Al_2O_3 is reported in Figure 5.9. NH_3 TPD gives rise to a low temperature peak, with a maximum at 125°C, and a shoulder at 200°C, with a tail extending to 600°C. The spectrum points to a wide distribution of strengths of acid sites. The total amount of desorbed ammonia is 7.2×10^{-5} mole/g of catalyst, corresponding to 1.6×10^{17} molecule/m^2 of catalyst.

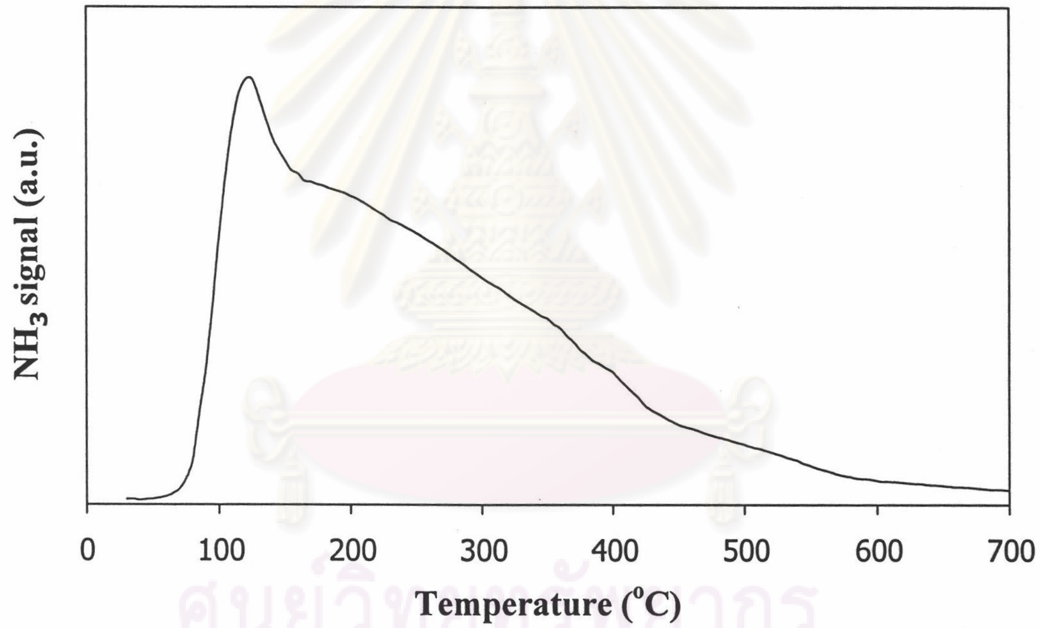

Figure 5.9 Ammonia TPD spectrum of a Pt/Al_2O_3 catalyst

5.2.4 Basicity Behavior

In fact, the surface basicity of Al_2O_3-based catalysts is fairly important on a catalytic and a conventional chemical ground, for their acidity rather than for their basicity. However, some literature [214] has reported the promotional effect of alkalis, which are relatively concerned with the surface basicity, on the catalytic reduction of NO by propene over Pt-based catalyst. Hence, the surface basicity is measured by the gas-solid adsorption and desorption of CO_2 method in this section. Figure 5.10 exhibits CO_2 TPD profile of 1 %wt Pt/Al_2O_3 catalyst. This spectrum shows a peak with a maximum at 100°C and a long tail, extending to 450°C. The total amount of desorbed carbon dioxide is approximately 1.0×10^{-5} mole/g of catalyst, corresponding to 2.2×10^{16} molecule/m^2 of catalyst.

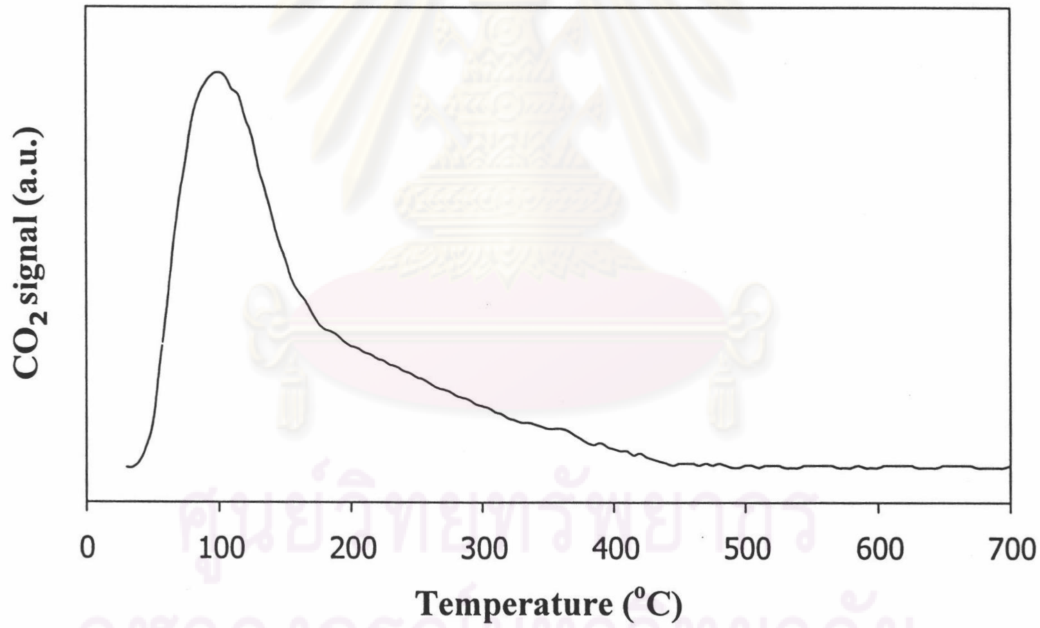

Figure 5.10 Carbon dioxide TPD spectrum of a Pt/Al_2O_3 catalyst

5.3 Mechanistic Studies in the Selective Catalytic Reduction of NO by C_3H_6 under Excess Oxygen on a Pt/Al_2O_3 Catalyst through the Investigation of Surface Species

5.3.1 The Catalytic Activity Behavior

The general feature for the selective catalytic reduction of NO by C_3H_6 is the competitive interaction between NO and O_2 to selectively react with C_3H_6. Although this reaction operates under a large excess of oxygen, NO, which is present even at a much lower concentration than O_2, can effectively react with C_3H_6. Hence, the surface oxygen is expected to be more important in the reaction than the gas phase oxygen. Two sets of Pt/Al_2O_3 catalyst on which the different surface oxygen was prepared by the two different pretreatments were tested by the catalytic activity measurement toward temperature programmed reaction to justify this. The first type of surface oxygen on a Pt/Al_2O_3 catalyst was obtained from the calcination in air. This sample is labeled to be Pt_{ox}/Al_2O_3 catalyst. Another surface oxygen was produced from the reoxidation of a Pt_{ox}/Al_2O_3 catalyst pre-reduced under hydrogen flow and this sample is denoted to be Pt_{red}/Al_2O_3 catalyst. The characteristic of surface oxygen on non-reduced Pt/Al_2O_3 catalyst was proved to be certainly different from that on pre-reduced Pt/Al_2O_3 catalyst in reference [215].

Figure 5.11 shows the comparison of temperature programmed reaction profile involving C_3H_6 and NO conversions versus the elevated temperature between Pt_{ox}/Al_2O_3 and Pt_{red}/Al_2O_3 catalysts. Both catalysts show the same catalytic activity behavior although the profiles of C_3H_6 and NO conversions for Pt_{ox}/Al_2O_3 catalyst appear at higher temperature ranges compared with those for Pt_{red}/Al_2O_3 catalyst. The NO reduction reaches a sharp maximum of approximately 40% at 275°C and 15% at 375°C for Pt_{red}/Al_2O_3 and Pt_{ox}/Al_2O_3 catalysts, respectively. The onset of NO reduction and the peak in the NO conversion are closely related to the C_3H_6 oxidation. Conversions of C_3H_6 and NO begin at the same temperature and raise together until NO reduction reaches a maximum value at approximately similar temperature where the C_3H_6 oxidation is complete. This coincidence of C_3H_6 and NO conversions is a general phenomenon within lean-NO_x catalysis [116]. It is significantly noted that

Pt_{red}/Al_2O_3 catalyst gives much more N_2O selectivity than Pt_{ox}/Al_2O_3 catalyst. Therefore, in the NO reduction with C_3H_6 over Pt-based catalyst, the N_2O/N_2 ratio in the product depends much more strongly on temperature than the feature of surface oxygen.

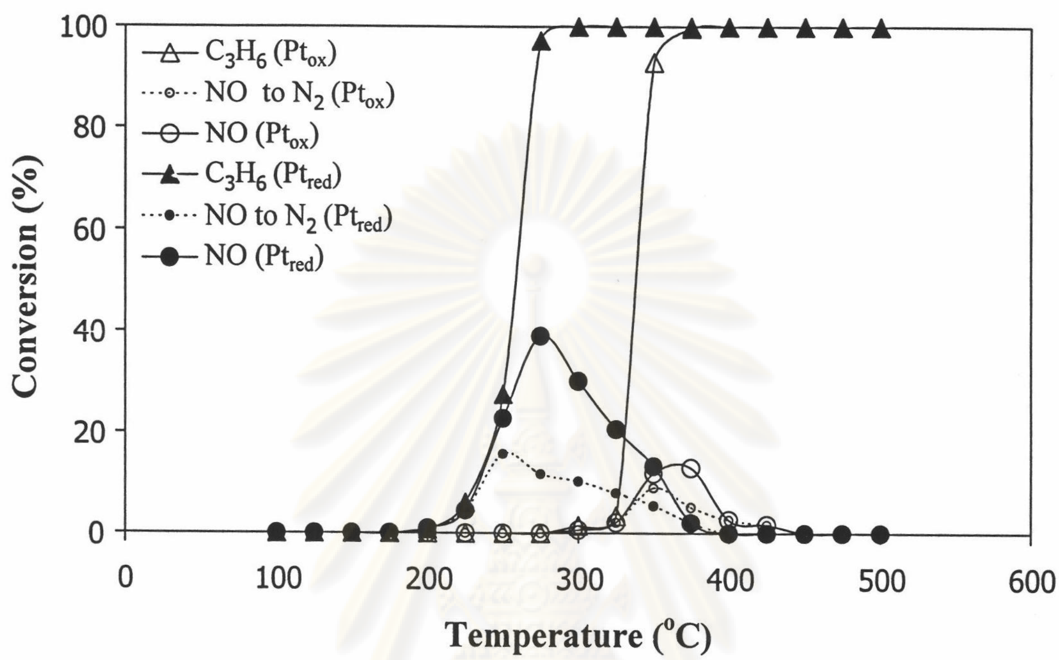

Figure 5.11 The temperature programmed reaction profiles of Pt_{ox}/Al_2O_3 and Pt_{red}/Al_2O_3 catalysts for the selective catalytic reduction of NO by C_3H_6 under excess oxygen

The maximum in the NO reduction curve can be attributed to the presence of two competing oxidation reactions between C_3H_6, and NO and O_2. At low temperatures below the temperature of maximum NO reduction C_3H_6 selectively reacts with NO. At temperatures above this temperature, however, the rate of the C_3H_6+O_2 reaction increases faster than the rate of C_3H_6+NO reaction, and as a result, decreased levels of NO reduction are observed. This is in agreement with the report that C_3H_6 and NO disappearance reactions have the same activation energy values at low reaction temperatures whereas C_3H_6 and O_2 have the same activation energy values at high reaction temperatures [189]. The close coupling between the NO reduction and the C_3H_6 oxidation curves at temperatures below the temperature of maximum NO reduction suggests that the activation of the hydrocarbon is kinetically significant in this region. It is suggested that the C_3H_6 activation on Pt_{red}/Al_2O_3

catalyst occurs faster than that on Pt_{ox}/Al_2O_3 catalyst resulting in lowering the onset reaction temperature. The capability in hydrogen consumption at lower temperatures of pre-reduced Pt/Al_2O_3 catalyst in other literature [216] supports this speculation.

The effect of the presence of NO on the C_3H_6 oxidation activity of Pt_{ox}/Al_2O_3 and Pt_{red}/Al_2O_3 catalysts was also examined. On both catalysts the presence of NO retards the activation of C_3H_6 by 100°C, as can be seen in Figure 5.12. This result is corresponding with the reference suggesting that at low temperatures NO blocked the active sites responsible for propene oxidation [120]. It should be noted that the inhibition of C_3H_6 oxidation activity by NO is independent on the different feature of surface oxygen.

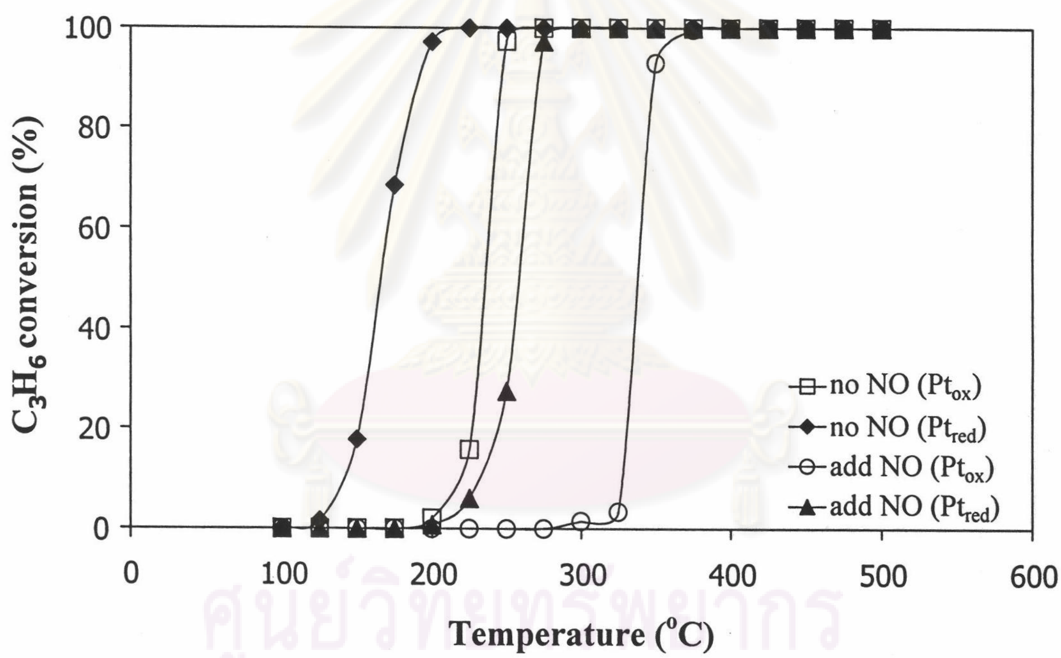

Figure 5.12 Effect of the presence of NO on C_3H_6 oxidation activity on Pt_{ox}/Al_2O_3 and Pt_{red}/Al_2O_3 catalysts

5.3.2 The Nature of Surface Species

To approach the main goal for proposal of reaction mechanism, the detailed information about the feature of surface species produced on the catalyst surface is enough obtained and carefully considered because the surface species behave to be not only the intermediate species but also the spectator species. Although the use of *in situ* Fourier transform infrared spectroscopy technique seems to be still the routine way to evaluate an exact role of surface species, the contradictory conclusions in the published works have been regularly occurred. Therefore, the proposed reaction mechanism related to the claimed intermediate species is also ambiguous. Hence, the other procedures are necessarily proposed to support and confirm the previous information from IR technique. In this part, the characterization of surface species was conducted by an experimental set containing three continuous steps containing reaction step, temperature programmed desorption (TPD) step and temperature programmed oxidation (TPO) by O_2 step. During the first step, the sample was exposed to the selected reactant gas mixture at a given temperature until saturation for producing the surface species. It is noted that the steady state conversions were obtained by this step. The TPD experiment on the second step was subsequently carried out to remove the adsorbed surface species. Afterwards, the removal of the remaining deposits was performed in the final step.

Prior to study the reaction mechanism of the selective catalytic reduction of NO by C_3H_6 under lean-burn condition via the investigation of surface species by the temperature programmed technique, such technique is employed with the reaction involving the well know mechanism in order to prove that this technique can be effective for the prediction of reaction mechanism. Co-ZSM-5 is an attractive catalyst because its activity for the selective catalytic reduction of NO by methane is very high, compared to other ion-exchanged ZSM-5 catalysts. Although the introduction of the other hydrocarbons instead of methane has not much been studied, the previous works have been unanimous that the proposed mechanism for the selective catalytic reduction of NO by various hydrocarbons over Co-ZSM-5 is the same pathway. It contains two main steps, i.e., the hydrocarbon activation leading to the N-containing intermediate species and the conversion of these species to final products.

From the observation about the formation of intermediate species on Co-ZSM-5 by varying the adsorbed gas mixture in absorption step (C_3H_6, C_3H_6+NO, $C_3H_6+O_2$ and $C_3H_6+NO+O_2$), it is found that for all systems the surface species are entirely removed on TPO step, while no species was released during TPD step. In addition, it can be concluded that the intermediate species for the selective catalytic reduction of NO by propene on Co-ZSM-5 catalyst are necessarily formed by the interaction of NO, propene and oxygen. The investigation of the removal of intermediate species for the selective catalytic reduction of NO by propene in the presence of oxygen excess over Co-ZSM-5 by varying oxidizing gases (NO, O_2 and NO+O_2) indicates that the cooperation of NO and oxygen possibly accelerated the removal of intermediate species. These results are in agreement with the open literatures [217-219] reporting the reaction mechanism; therefore, the temperature programmed technique is definitely confirmed to use for the prediction of reaction mechanism.

First, the influence of NO on the formation of surface species over Pt/Al_2O_3 is studied to prove how the inhibition of propene activation by NO is occurred. Due to the similarity of catalytic activity behavior for both Pt_{ox}/Al_2O_3 and Pt_{red}/Al_2O_3 catalysts only one is tested. Pt_{red}/Al_2O_3 catalyst is chosen because it is easy to observe NO conversion. Two sets of gas mixture ($C_3H_6+O_2$ and $C_3H_6+NO+O_2$) were used in the first step at 100°C to produce the surface species. It is noted that at this temperature no conversion is noticed. Figures 5.13 and 5.14 depict the relevant traces of outlet gases obtained on TPD step after dosing the gas mixture of $C_3H_6+O_2$ and $C_3H_6+NO+O_2$ on Pt_{red}/Al_2O_3 catalyst, respectively. The main outlet gases for $C_3H_6+NO+O_2$ system are carbon dioxide and nitrogen, while only carbon dioxide is released when there is no NO in the adsorbed gas mixture. It is significantly noticed that no species is detected during TPO step.

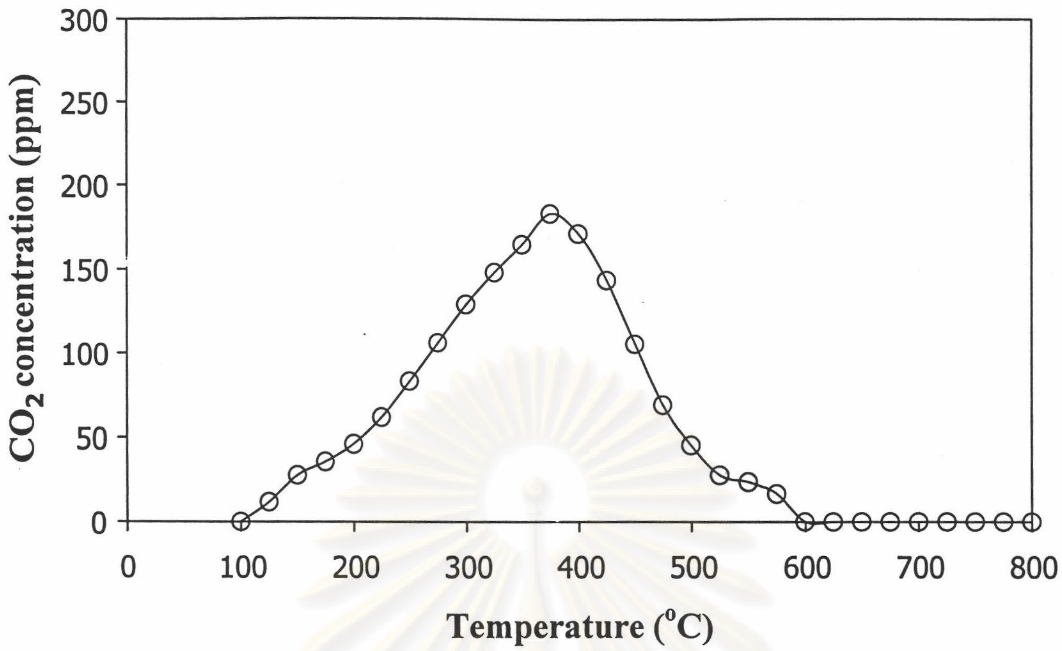

Figure 5.13 The temperature programmed desorption profile of Pt_{red}/Al_2O_3 after dosing 1000 ppm C_3H_6 + 5% O_2 at 100°C for 2 h

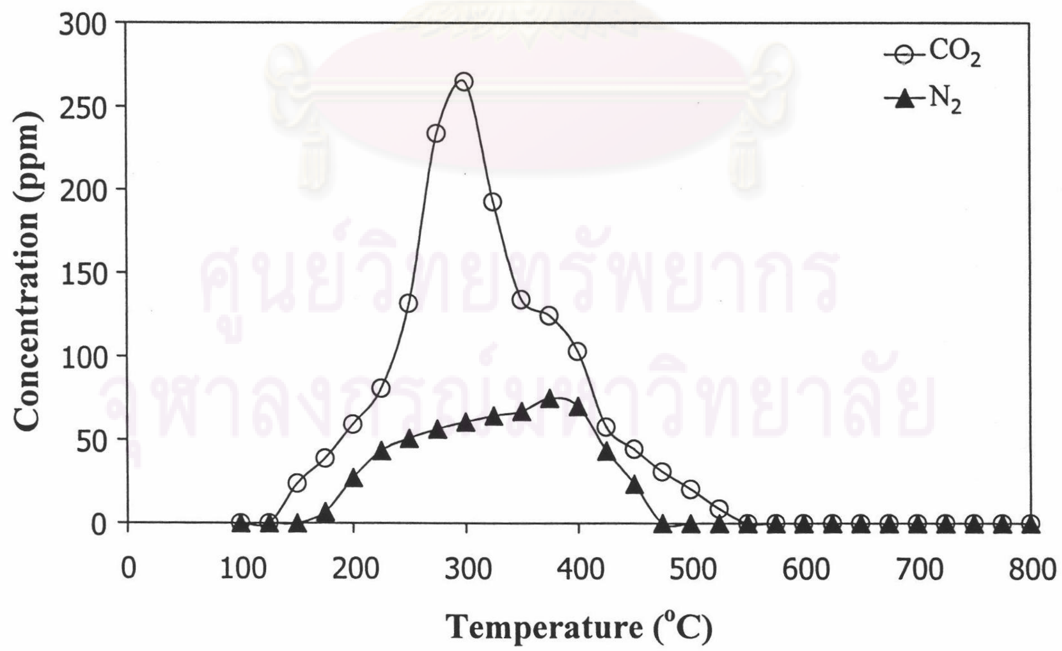

Figure 5.14 The temperature programmed desorption profiles of Pt_{red}/Al_2O_3 after dosing 1000 ppm C_3H_6 + 1000 ppm NO + 5% O_2 at 100°C for 2 h

For C_3H_6+O_2 system, a sharp peak of carbon dioxide appears at 375°C whereas for C_3H_6+NO+O_2 system, it is shifted to lower temperature (at approximately 300°C) with a shoulder at ca. 375°C. It is noted that the amount of carbon-containing compounds released from both systems is equivalent. Taking close consideration, it is seen that there are two peaks in C_3H_6+NO+O_2 system after deconvolution, i.e., at 300 and 375°C. In addition, the deconvolution of nitrogen profile obtained from C_3H_6+NO+O_2 system shows a peak at 375°C and a broad peak at low temperature range (200-350°C). From these results, it is inclined that the presence of NO in the adsorbed gas mixture induces nitrogen containing surface species at 300°C. According to the open literatures [124, 125], nitro and nitrito organic compounds were absolutely detected by DRIFTS after addition of a mixture of C_3H_6+NO+O_2 onto Pt-ZSM-5 at 100°C. The coincident position of carbon dioxide peak at 375°C in both systems and the appearance of nitrogen peak at the same temperature for C_3H_6+NO+O_2 system may imply two aspects. First, these carbon dioxide peaks at 375°C represent to the same type of surface species whereas nitrogen peak is occurred due to the decomposition of adsorbed NO. Second, types of surface species for two systems are different but their partial structures may be similar.

However, the nature of surface species can be certainly changed under the reaction condition. The earlier work found that for the reaction of C_3H_6+NO_2+O_2 on Pt/SiO_2, the organic nitro and nitrite compounds appeared at low temperature whereas the organic carbonyl species and isocyanate species occurred at higher temperature [123]. Therefore, the surface species over Pt_{red}/Al_2O_3 are also observed after dosing the gas mixture of C_3H_6+O_2 and C_3H_6+NO+O_2 at each reaction temperature of 150°C and 225°C, respectively. At a given temperature, C_3H_6 conversion of each system is equally approximately 20%. Figures 5.15 and 5.16 illustrate the traces of outlet gases during TPD step containing carbon dioxide, methane, carbon monoxide and oxygen for C_3H_6+O_2 system and the additional nitrogen and nitrous oxide for C_3H_6+NO+O_2 system. It is significantly remarked that most of surface species are released during TPD step whereas the amount of outlet gases by TPO step is extremely small. Hence, it is suggested that the surface species can easily decompose themselves on Pt_{red}/Al_2O_3 catalyst, unlike zeolite-based catalyst as reported elsewhere [220].

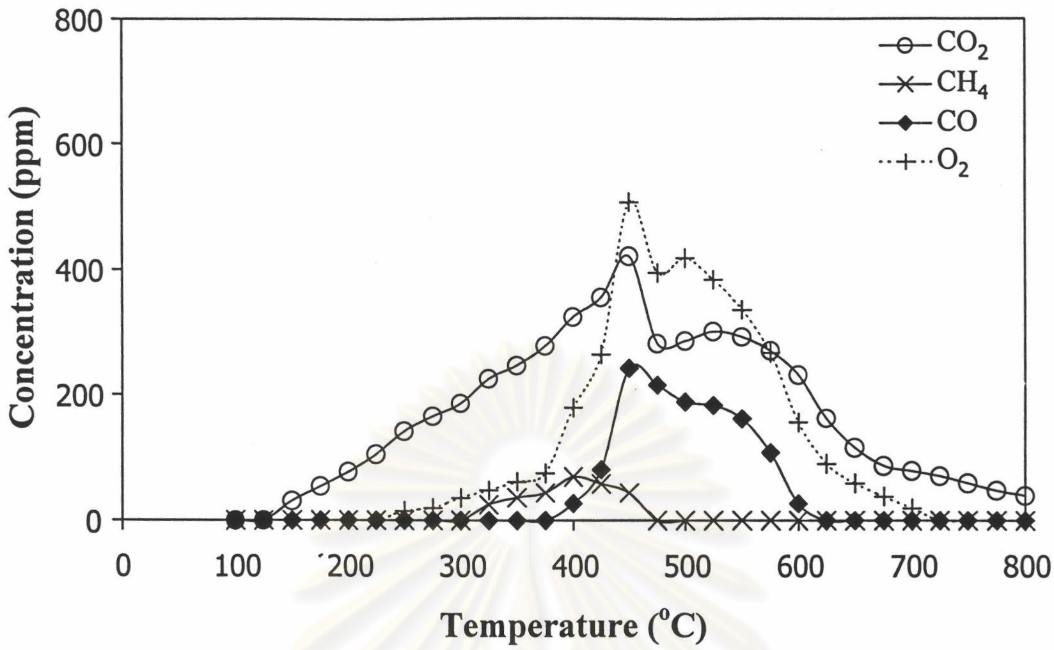

Figure 5.15 The temperature programmed desorption profiles of Pt_{red}/Al_2O_3 after dosing 1000 ppm C_3H_6 + 5% O_2 at 150°C for 2 h

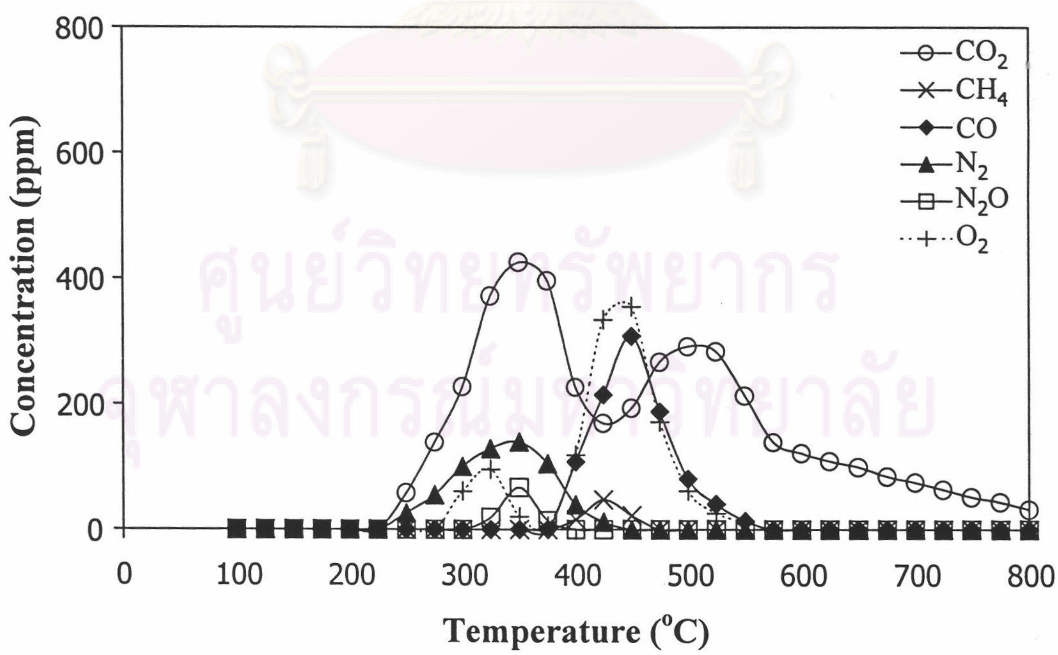

Figure 5.16 The temperature programmed desorption profiles of Pt_{red}/Al_2O_3 after dosing 1000 ppm C_3H_6 + 1000 ppm NO + 5% O_2 at 225°C for 2 h

In case of C_3H_6+O_2 system, as seen in Figure 5.15, the carbon dioxide profile shows two main peaks at 450°C and 525°C. There is a little amount of methane at a temperature range 300°C to 475°C. It was interesting that for the carbon monoxide and oxygen traces, their peak and shoulder are located to be coincident with the carbon dioxide peak at 450°C and that at 525°C, respectively. In case of C_3H_6+NO+O_2 system as shown in Figure 5.16, there are two carbon dioxide peaks and two oxygen peaks in TPD profile, while the other gases give only one peak. Nitrogen and nitrous oxide peaks exist at low temperature whereas methane and carbon monoxide peaks are located at higher temperature. The deconvolution of these TPD profiles indicates that there are at least three types of surface species occurred on the catalyst surface. They are addressed as $C_xH_yO_zN_w$, $(C_iH_jO_k)_{LT}$, and $(C_lH_mO_n)_{HT}$ species decomposing themselves at low temperature region (200°C to 400°C), at moderate one (350°C to 550°C) and at high one (400°C to 800°C), respectively. The existence of these surface species is in agreement with the observation by IR technique in several references [121-127]. An example involves the observation of cyanide, isocyanate, acetate, and formate species on Pt/Al_2O_3 in C_3H_6+NO+O_2 system by the use of *in situ* Fourier transform infrared spectroscopy [126]. It was also found that only isocyanate species disappeared by flushing with helium at 250°C. In addition, only isocyanate and acetate species were observed when increasing the reaction temperature at 350°C and again only the intensity of isocyanate peak was essentially affected after the reactor was flushed with helium.

Considering the feature of surface species obtained by dosing the gas mixture of C_3H_6+O_2 at 150°C, the position of both carbon dioxide peaks is definitely coincident with that of two TPD peaks assigned as $(C_iH_jO_k)_{LT}$, and $(C_lH_mO_n)_{HT}$ species in C_3H_6+NO+O_2 system. From this result, it is believed that NO assisted the production of the particular surface species assigned as $C_xH_yO_zN_w$ species whereas two types of partially oxidized hydrocarbons, $(C_iH_jO_k)_{LT}$, and $(C_lH_mO_n)_{HT}$ species, are certainly generated in both C_3H_6+O_2 and C_3H_6+NO+O_2 systems.

In fact, the obtained surface species may possibly play a role to be either the intermediate species or the spectator species depending on the reaction condition as reported in some literature. An example of the contradictory proposal is that nitro, nitrite and carbonyl surface species were proposed to be key reaction intermediates for the selective catalytic reduction of NO by C_3H_6 on Pt/SiO_2 at 120°C in one published paper [121]. While the other works suggested that nitro, nitrito and isocyanate species were not the catalytic active intermediates for the selective catalytic reaction of NO by C_3H_6 on Pt-ZSM-5 at 250°C [124, 125]. In addition, there is some literature concluding independently that carboxylates, nitrates and cyanide species were probably the spectator byproducts of the selective catalytic reduction of NO by C_3H_6 on Pt/Al_2O_3 at 250°C, whereas the surface isocyanate species could be a potential reaction intermediate in such reaction [126]. With the above-mentioned reason, the reactivity of $C_xH_yO_zN_w$, $(C_iH_jO_k)_{LT}$, and $(C_lH_mO_n)_{HT}$ species with the oxidizing reactant gas in the reaction temperature range is also studied. The reactivity test was conducted by using TPO technique after the production of surface species through dosing gas mixtures of C_3H_6+O_2 and C_3H_6+NO+O_2 on Pt_{red}/Al_2O_3 at 150 and 225°C, respectively. Two sets of the oxidizing gases were varied as 1% O_2 and the gas mixture of 1000 ppm NO and 1% O_2. It was noted that the TPD step was negligible in this reactivity test.

Figures 5.17 and 5.18 show the traces of outlet gases obtained from the oxidation of surface species by O_2 over Pt_{red}/Al_2O_3 catalyst, which is exposed by C_3H_6+O_2 and C_3H_6+NO+O_2 mixtures, respectively. These outlet gases contain carbon dioxide, nitrogen and nitrous oxide for C_3H_6+NO+O_2 system and only carbon dioxide is released from the catalyst surface for C_3H_6+O_2 system. With the surface species produced by C_3H_6+NO+O_2 mixture, it is found that the position of carbon dioxide peak addressed as $C_xH_yO_zN_w$ species was unaffected with introducing O_2 as oxidizing gas. Furthermore, the positions of nitrogen and nitrous oxide peaks are also not shifted with increasing temperature. This result reveals that $C_xH_yO_zN_w$ species can decompose themselves under a large excess of oxygen at the same temperature where they decompose under helium flow. Considering the reactivity behavior with O_2 of $(C_iH_jO_k)_{LT}$, and $(C_lH_mO_n)_{HT}$ species for both dosing gases through the carbon dioxide peak, the same pattern of carbon dioxide curves is observed. A larger amount of carbon dioxide released at low temperature and the disappearance of the carbon dioxide peak at high temperature (525°C) indicates that the surface species decomposing at high temperature, $(C_lH_mO_n)_{HT}$ species, are easily removed by O_2.

However, the relatively small shift to lower temperature of the peak of $(C_iH_jO_k)_{LT}$ species and neither methane nor carbon monoxide released from the catalyst surface manifest that these species are slightly reactive with O_2. It is remarked that $(C_iH_jO_k)_{LT}$ species obtained from C_3H_6+O_2 mixture is more easily oxidized by O_2 than those obtained from C_3H_6+NO+O_2 mixture. It may be due to the different chemical proportion of C, H and O atoms in $(C_iH_jO_k)_{LT}$ species of both systems.

When the oxidizing gas is changed from O_2 to NO+O_2, the concentrations of carbon and nitrogen containing compounds removed during TPO experiment for using C_3H_6+O_2 and C_3H_6+NO+O_2 mixtures as the dosing gases are illustrated in Figures 5.19 and 5.20, respectively. It is observed that using either O_2 or NO+O_2 as the oxidizing gas the patterns of carbon dioxide curves are rather similar in each system. However, the significant differences of two oxidizing gases are the additional production of nitrogen in C_3H_6+O_2 system and the larger amount of nitrogen in C_3H_6+NO+O_2 system for using NO+O_2 instead of O_2. This indicates the interaction between $(C_iH_jO_k)_{LT}$, as well as $(C_lH_mO_n)_{HT}$ species and NO to produce nitrogen but this phenomena hardly influence the oxidation of these partially oxidized hydrocarbon by O_2. This corresponds with the earlier literature [121], which suggested that on Pt/SiO_2 the carbonyl species reacted rapidly with NO_2 and O_2 at 120°C. On the other hand, with the reactivity of $C_xH_yO_zN_w$ species, it is confirmed that these species still decompose themselves under the oxidizing atmosphere even adding a small amount of NO due to no shift of carbon dioxide peak at 350°C and the nitrous oxide peak at the same temperature. Nevertheless, the observation of nitrogen peak at 350°C is rather difficult under NO+O_2 atmosphere because nitrogen atoms in the oxidizing gas could possibly interact with other surface species to produce nitrogen. However, no shift of nitrogen peak in the introduction of only O_2 during TPO experiment can eliminate this doubtfulness. Therefore, it is pronounced that neither NO nor O_2 is involved in the decomposition of $C_xH_yO_zN_w$ species at any temperature. This was also in agreement with the previous work [126] reporting that the surface cyanide on Pt/Al_2O_3 was not reacting in NO, NO_2, O_2 and NO+O_2 environments at 250°C.

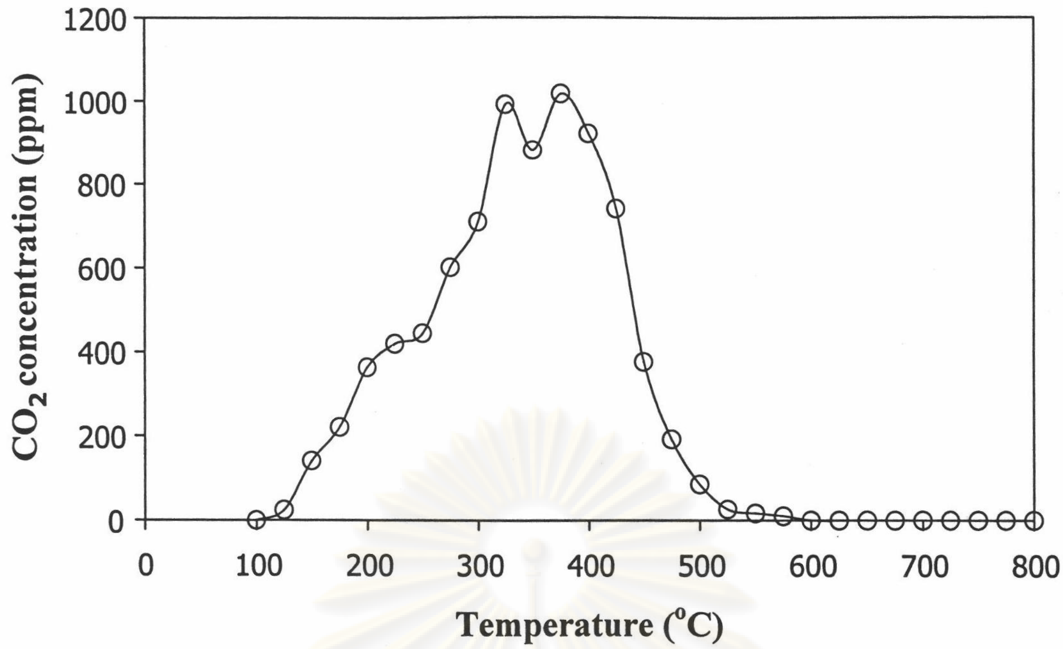

Figure 5.17 The temperature programmed oxidation profiles of Pt_{red}/Al_2O_3 by using 1% O_2 as the oxidizing gas after dosing 1000 ppm C_3H_6 + 5% O_2 at 150°C for 2 h

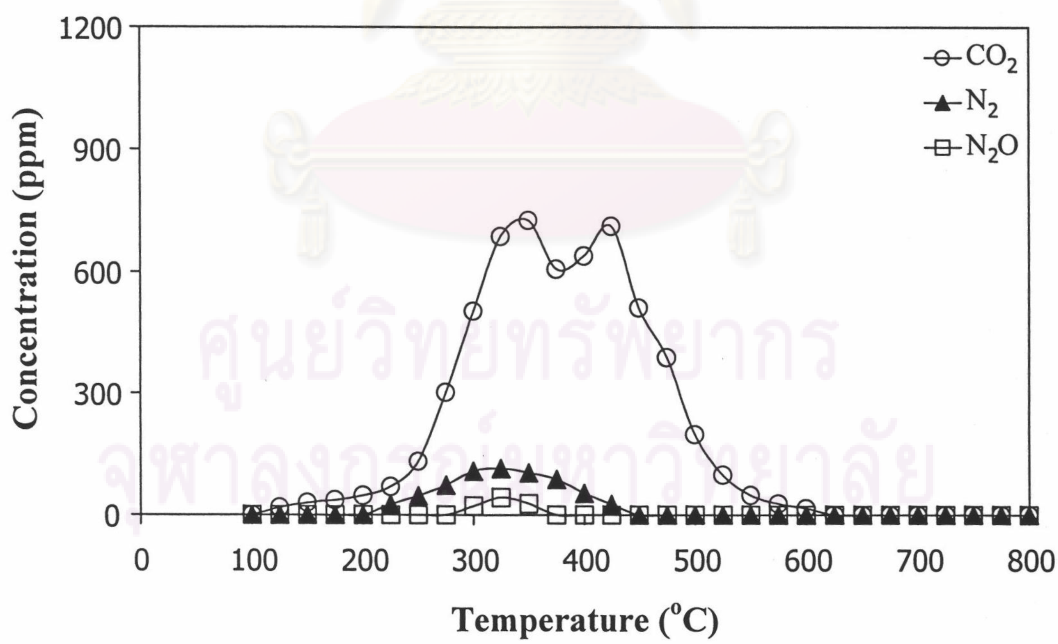

Figure 5.18 The temperature programmed oxidation profiles of Pt_{red}/Al_2O_3 by using 1% O_2 as the oxidizing gas after dosing 1000 ppm C_3H_6 + 1000 ppm NO + 5% O_2 at 225°C for 2 h

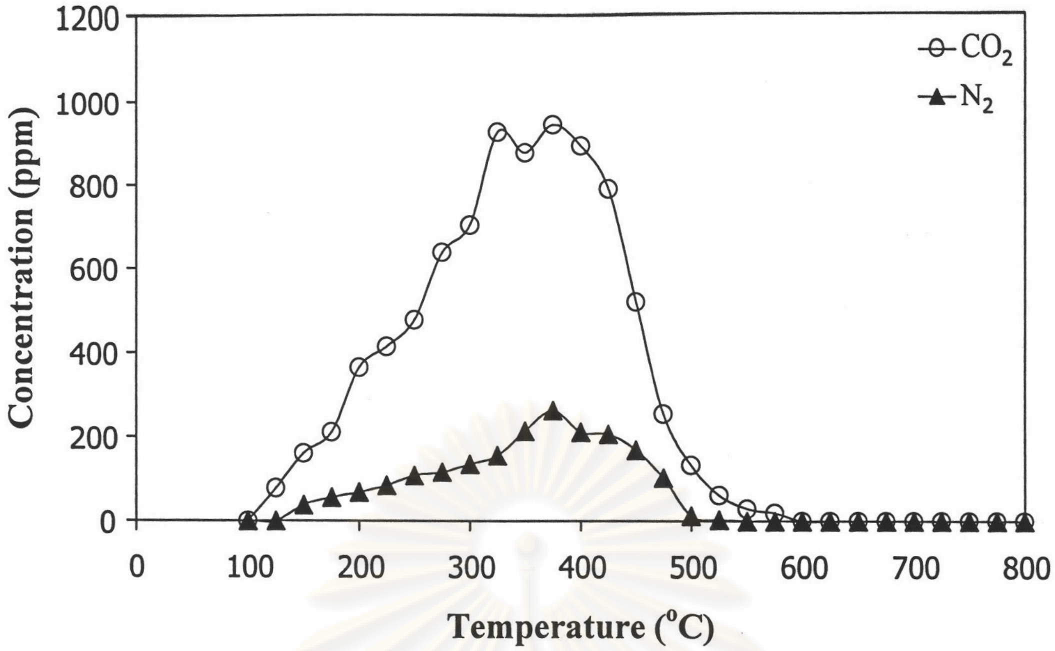

Figure 5.19 The temperature programmed oxidation profiles of Pt_{red}/Al_2O_3 by using 1000 ppm NO + 1% O_2 as the oxidizing gas after dosing 1000 ppm C_3H_6 + 5% O_2 at 150°C for 2 h

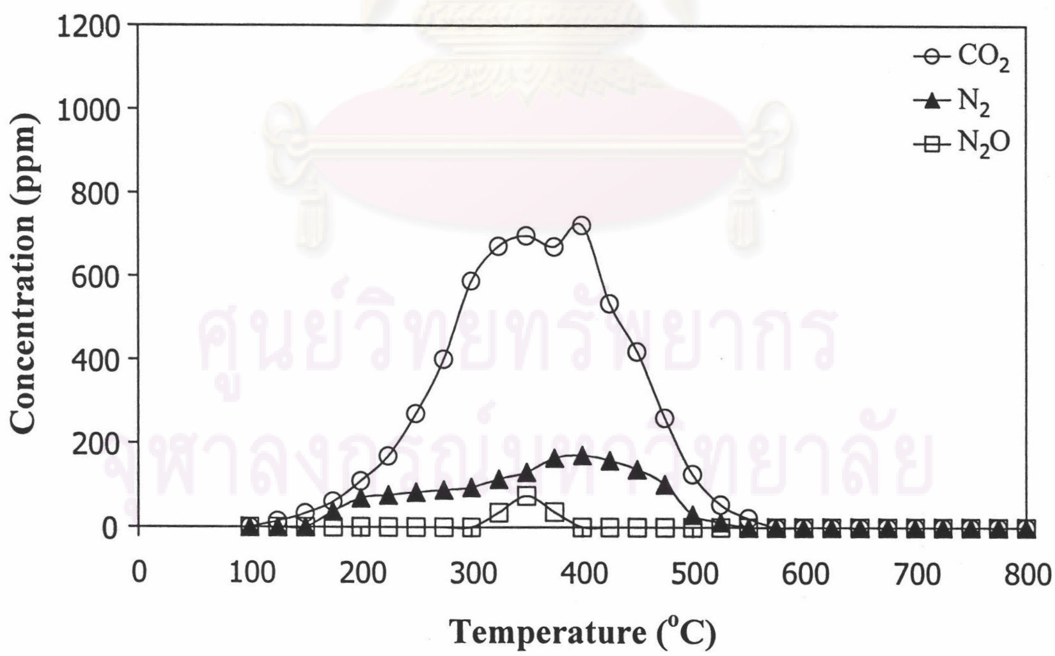

Figure 5.20 The temperature programmed oxidation profiles of Pt_{red}/Al_2O_3 by using 1000 ppm NO + 1% O_2 as the oxidizing gas after dosing 1000 ppm C_3H_6 + 1000 ppm NO + 5% O_2 at 225°C for 2 h

From the observation in the reactivity test by $NO+O_2$ that NO can react with two partially oxidized hydrocarbon to produce nitrogen under a large excess of oxygen, it is interesting to prove whether only NO can react with these species. Figure 5.21 demonstrates the temperature programmed oxidation profile of Pt_{red}/Al_2O_3 catalyst after dosing $C_3H_6+NO+O_2$ mixture at 225°C for 2 h followed the elevation of temperature under NO atmosphere. It is clear that the peaks of three carbon containing products are still in the same position compared with those obtained from the elevation of temperature under helium atmosphere. However, under NO atmosphere the carbon monoxide peak addressed as $(C_iH_jO_k)_{LT}$ species is properly substituted by the carbon dioxide peak. This shows the slight reactivity of $(C_iH_jO_k)_{LT}$ species to NO. The large production of nitrogen containing products indicates that NO can independently react with three surface species at each decomposing temperature of them. Importantly, it should be noted that the existence of carbon dioxide peak at 525°C in case that only NO is used as the oxidizing gas exhibits that O_2 is a more potential oxidizing gas than NO to be reactive with $(C_lH_mO_n)_{HT}$ species. Also, the nitrogen product detected at low temperature range under $NO+O_2$ atmosphere is not produced from the direct interaction between NO and $(C_lH_mO_n)_{HT}$ species but the reaction between NO_2 favored by NO oxidation at low temperature and these species. This is in agreement with the earlier work [121], which reported that on Pt/SiO_2 the carbonyl species reacted rapidly with NO_2 at 120°C but they were inactive to NO at the same temperature.

From all above information about the feature of surface species produced from the reactant with NO and without NO, it can concluded that NO does not affect the formation of partially oxidized hydrocarbons as well as their reactivity to oxidizing gases but it assists to produce a new nitrogen containing species, which can decompose themselves at low temperature. These nitrogen containing compounds may possibly involve the inhibition of C_3H_6 oxidation activity. In fact, the deceleration of C_3H_6 oxidation is not only occurred by the addition of NO but also by the change of the characteristic of surface oxygen. Hence, it is interesting to study the nature of surface species produced on Pt_{ox}/Al_2O_3 catalyst compared with that on Pt_{red}/Al_2O_3 catalyst.

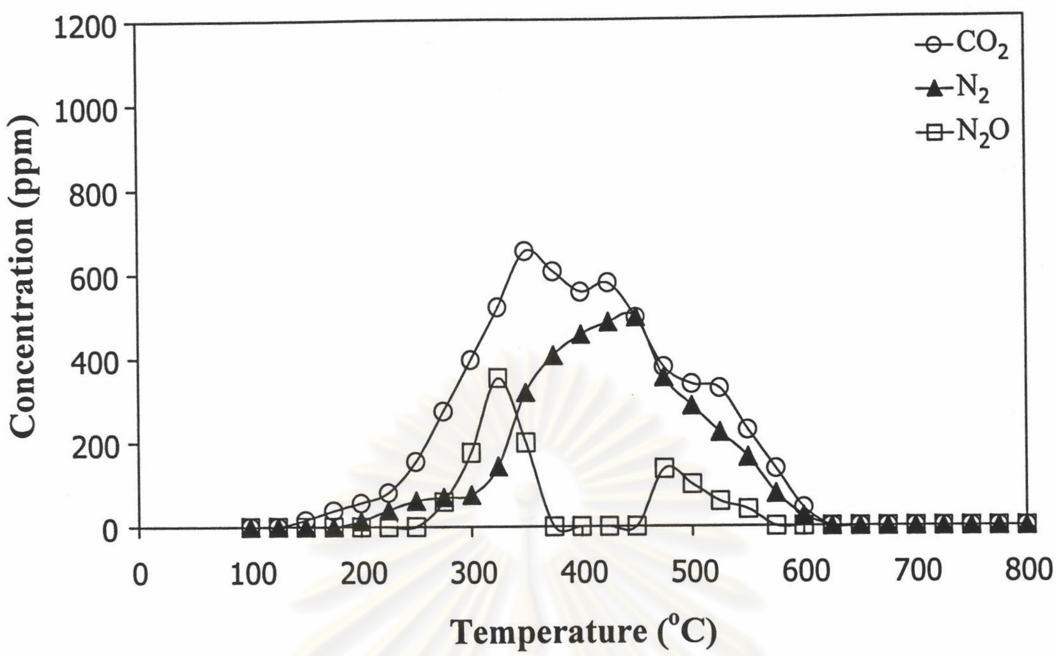

Figure 5.21 The temperature programmed oxidation profiles of Pt_{red}/Al_2O_3 by using 1000 ppm NO as the oxidizing gas after dosing 1000 ppm C_3H_6 + 1000 ppm NO + 5% O_2 at 225°C for 2 h

Figure 5.22 shows the traces of outlet gases during TPD step containing carbon dioxide, methane, carbon monoxide, oxygen, nitrogen and nitrous oxide after dosing the mixture of C_3H_6+NO+O_2 over Pt_{ox}/Al_2O_3 catalyst at 325°C for 2 h. This TPD pattern is rather similar to that of Pt_{red}/Al_2O_3 catalyst. This indicates that all of surface species formed on Pt_{red}/Al_2O_3 catalyst are also generated over Pt_{ox}/Al_2O_3 catalyst. Hence, the inhibition of C_3H_6 oxidation activity due to the change of surface oxygen indirectly involves types of surface species, unlike the presence/absence of NO. The reactivity test to O_2 and NO+O_2 in this case is also conducted as illustrated in Figures 5.23 and 5.24, respectively. On the catalyst surface of Pt_{ox}/Al_2O_3 catalyst NO+O_2 mixture becomes a more potential oxidizing agent than O_2 to reactivate $(C_lH_mO_n)_{HT}$ species because of the large production of carbon dioxide at lower temperatures. This may be explained that NO in oxidizing gas mixture can interact with the surface oxygen over Pt_{ox}/Al_2O_3 catalyst to produce NO_2, which reacts more easily with the carbonacious species than only O_2 [221].

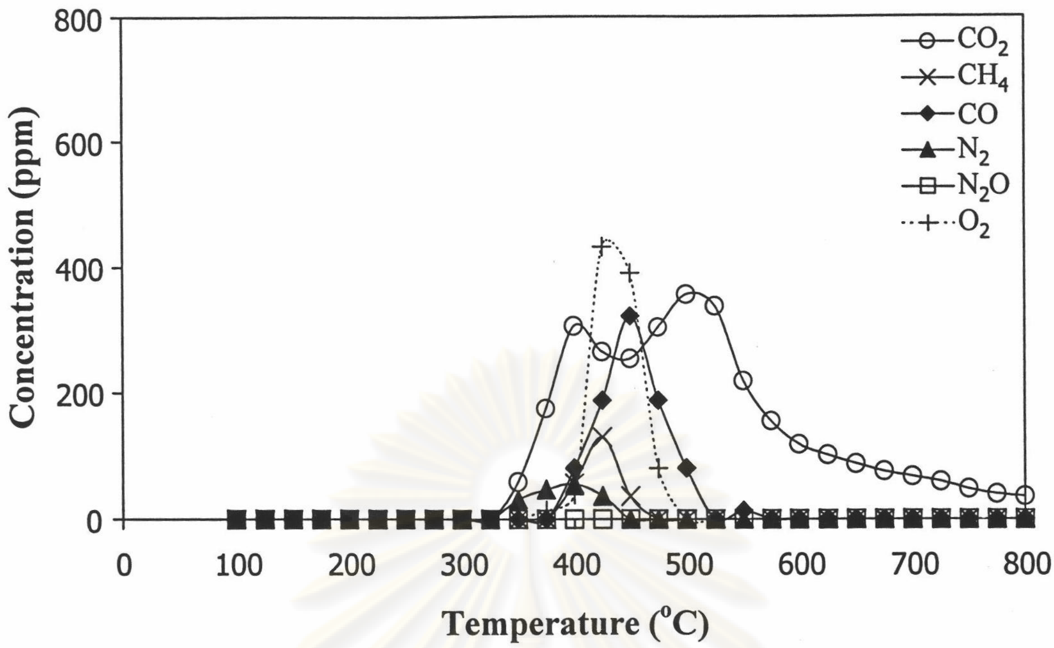

Figure 5.22 The temperature programmed desorption profiles of Pt_{ox}/Al_2O_3 after dosing 1000 ppm C_3H_6 + 1000 ppm NO + 5% O_2 at 325°C for 2 h

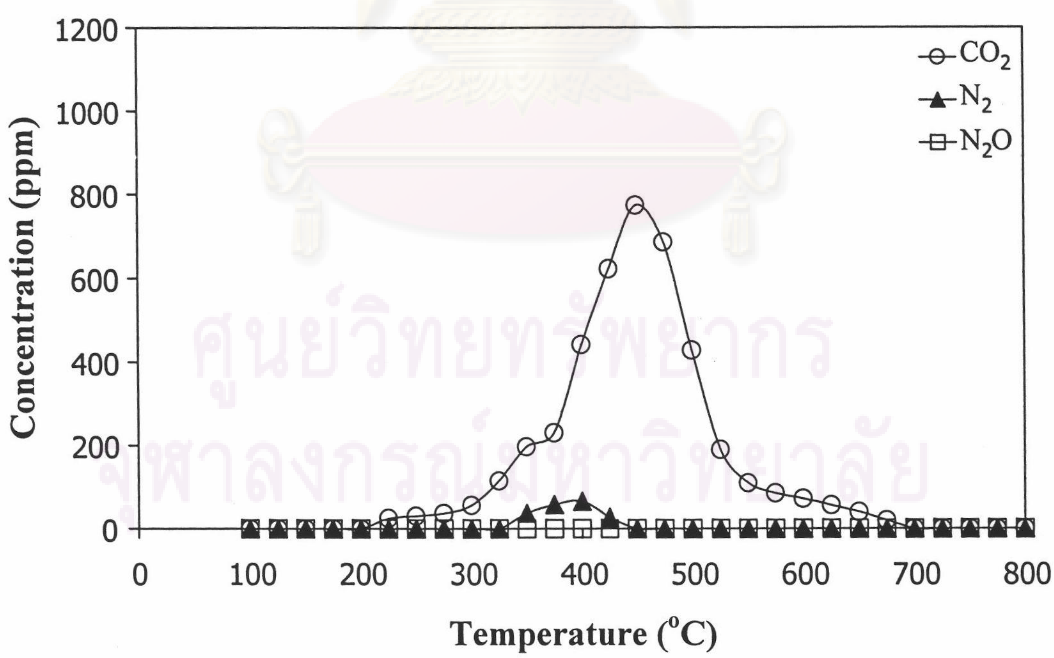

Figure 5.23 The temperature programmed oxidation profiles of Pt_{ox}/Al_2O_3 by using 1% O_2 as the oxidizing gas after dosing 1000 ppm C_3H_6 + 1000 ppm NO + 5% O_2 at 325°C for 2 h


1200

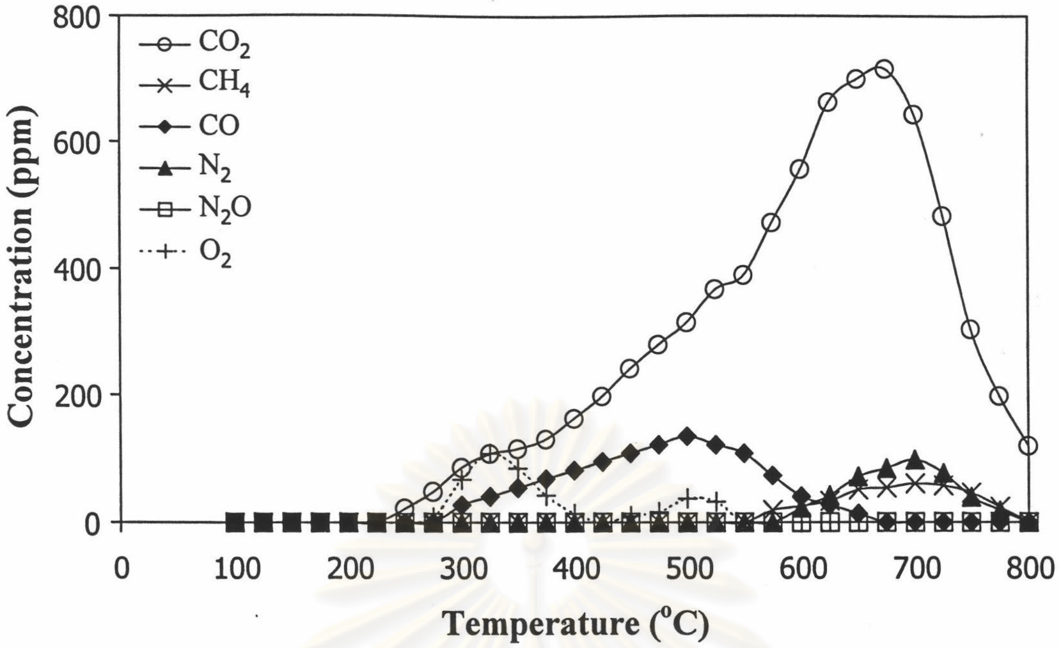

Figure 5.26 The temperature programmed desorption profiles of Pt_{red}/Al_2O_3 after dosing 1000 ppm C_3H_6 + 1000 ppm NO + 5% O_2 + 500 ppm SO_2 at 225°C for 2 h

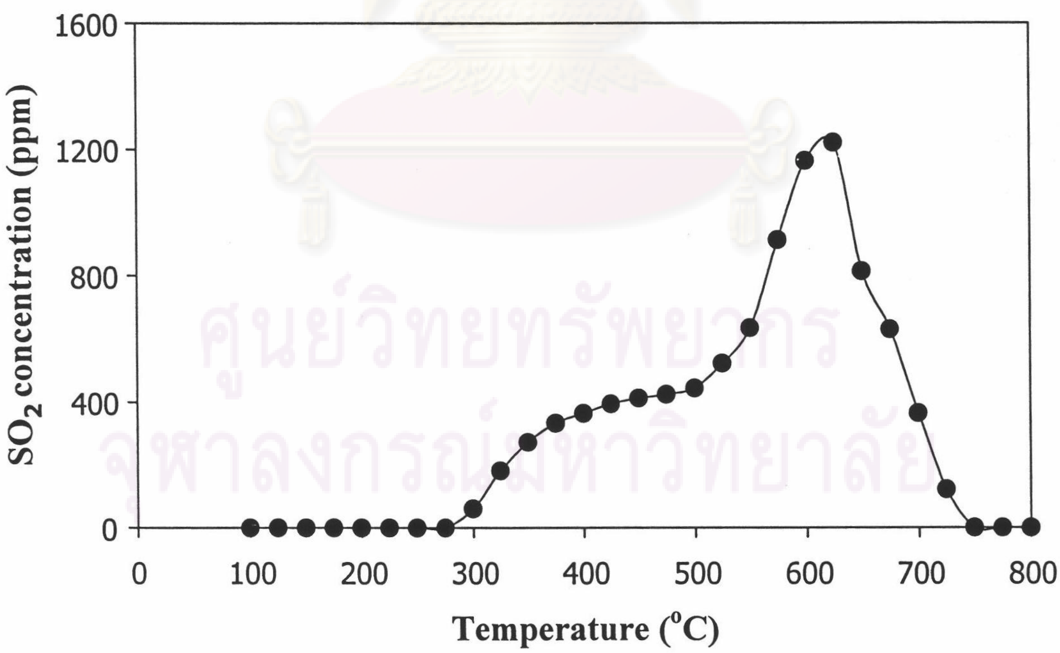

Figure 5.27 The sulfur dioxide concentration during the temperature programmed desorption profiles of Pt_{red}/Al_2O_3 after dosing 1000 ppm C_3H_6 + 1000 ppm NO + 5% O_2 + 500 ppm SO_2 at 225°C for 2 h

Due to the reversible inhibition of C_3H_6 and NO conversions by SO_2 the surface species after switching SO_2 out of the C_3H_6+NO+O_2 feed is taken close to the consideration. In the first step of an experimental set of three continuous steps the Pt_{red}/Al_2O_3 catalyst is first dosed by C_3H_6+NO+O_2+SO_2 mixture at 225°C for 1 h, immediately followed the switch of SO_2 out of the initial feed and subsequently held under the system without SO_2 at same temperature for 1 h. The temperature programmed desorption profile for this case is demonstrated in Figure 5.28 and the concentration of sulfur dioxide released during TPD step is separately shown in Figure 5.29. It is clear that $C_xH_yO_zN_w$ species is reproduced after switching SO_2 out of the feed due to the appearance of peaks of carbon dioxide and nitrogen at 350°C. The disappearance of broad peak, which is defined as adsorbed sulfur dioxide on Pt sites, at low temperature (300 to 400°C) indicates that SO_2 does not permanently modify the Pt surface. It is possible that adsorbed sulfur dioxide on Pt sites is substituted by $C_xH_yO_zN_w$ species and these species are therefore expected to occur on Pt sites as well. In addition, the carbon dioxide peak at 525°C assigned as $(C_lH_mO_n)_{HT}$ species is distinctly detected. The production of $C_xH_yO_zN_w$ species and the increase of $(C_lH_mO_n)_{HT}$ species coincident with the increase of C_3H_6 and NO conversions confirm the cooperation of $C_xH_yO_zN_w$ and $(C_lH_mO_n)_{HT}$ species directly involving the C_3H_6+NO+O_2 reaction. On the other hand, $(C_iH_jO_k)_{LT}$ species is again guaranteed to be the spectator species because of the decrease of carbon monoxide peak after switching SO_2 out of the system not relative to the increase of C_3H_6 and NO conversions. It is significantly noted that the surface sulphate species on Al_2O_3 representing a sharp peak of sulfur dioxide at 625°C are retained on the catalyst surface. This may ensure that the overall reaction mechanism for C_3H_6+NO+O_2 reaction proceeds on the only Pt surface, otherwise if Al_2O_3 support was cooperative to the reaction, the remaining surface sulphate species would inhibit C_3H_6 and NO conversions as found on C_3H_6+NO+O_2 system in elsewhere [134].

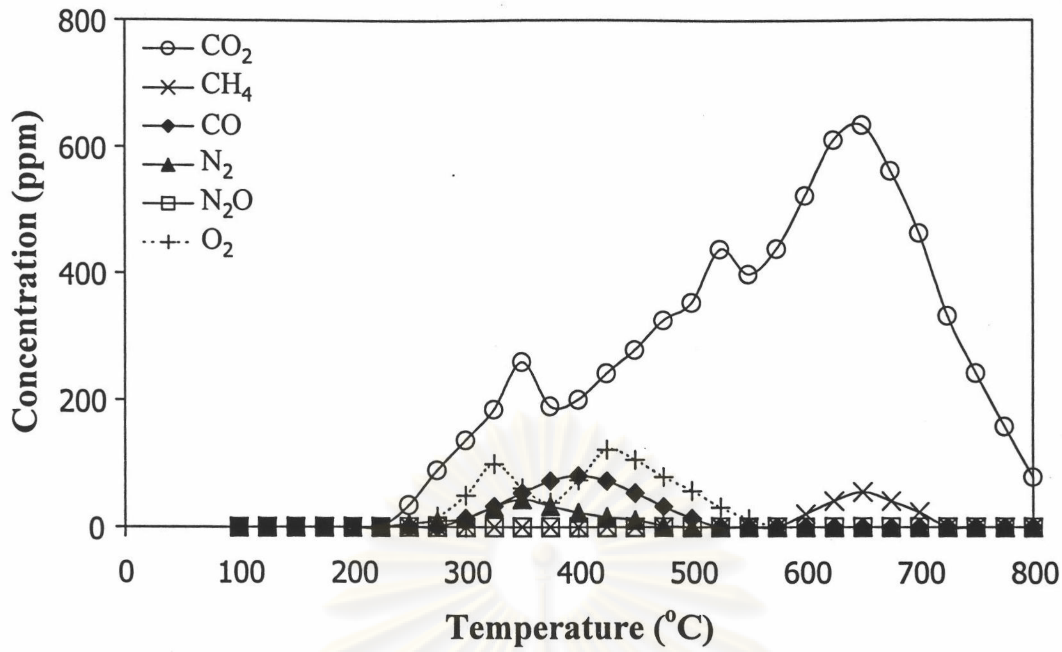

Figure 5.28 The temperature programmed desorption profiles of Pt_{red}/Al_2O_3 after dosing 1000 ppm C_3H_6 + 1000 ppm NO + 5% O_2 + 500 ppm SO_2 at 225°C for 1 h followed dosing 1000 ppm C_3H_6 + 1000 ppm NO + 5% O_2 at 225°C for 1 h

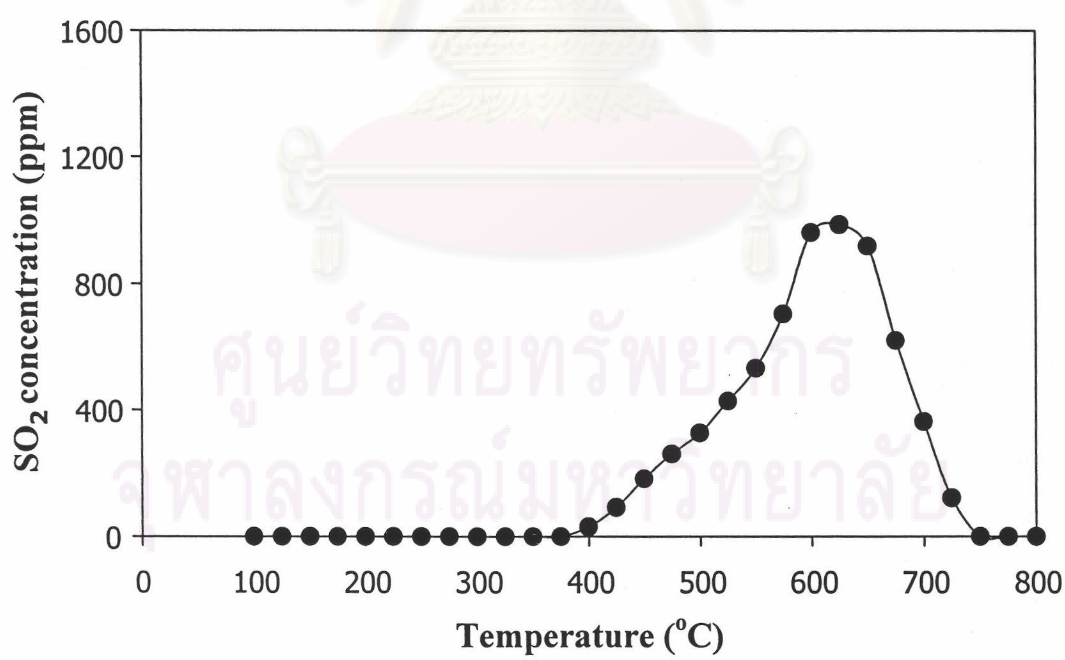

Figure 5.29 The sulfur dioxide concentration during the temperature programmed desorption profiles of Pt_{red}/Al_2O_3 after dosing 1000 ppm C_3H_6 + 1000 ppm NO + 5% O_2 + 500 ppm SO_2 at 225°C for 1 h followed dosing 1000 ppm C_3H_6 + 1000 ppm NO + 5% O_2 at 225°C for 1 h

5.3.4 The Proposed Mechanism

From the above results described in sections 5.3.2 and 5.3.3, the observation of three types of surface species indicates the complication in formation of surface species. Each surface species plays an independently different role on the overall reaction mechanism. It is postulated that there is at least three pathways following types of surface species in the overall reaction mechanism depending on the reaction temperature ranges. At low temperature ranges (150°C to 300°C), the NO reduction mechanism is mainly observed. $(C_lH_mO_n)_{HT}$ species on the catalyst surface easily react with either nitrogen dioxide or oxygen to produce nitrogen and carbon dioxide. The decomposition of $C_xH_yO_zN_w$ species occurs at moderate temperature ranges (200°C to 450°C). It is significantly remarked that the decomposition of $C_xH_yO_zN_w$ species is certainly attributed to produce nitrous oxide product. At high temperature ranges (350°C to 500°C), nitrogen dioxide and oxygen slightly assist to remove $(C_iH_jO_k)_{LT}$ species. However, the nitrogen production is still unclear. Two aspects should presumably explain this behavior. In the first case, NO could adsorb and decompose to nitrogen on vacant sites, which are occurred by the removal of $(C_iH_jO_k)_{LT}$ species. In the second case, nitrogen product is generated by the reaction between nitrogen dioxide and $(C_iH_jO_k)_{LT}$ species. It is noted that in fact, the latter reaction mechanism may be hardly occurred on Pt-based catalyst due to its activity being proceeded at low operating temperature in real condition. Hence, the mechanism for the selective catalytic reduction of NO by propene under oxygen excess on Pt/Al_2O_3 is proposed as shown in Figure 5.30.

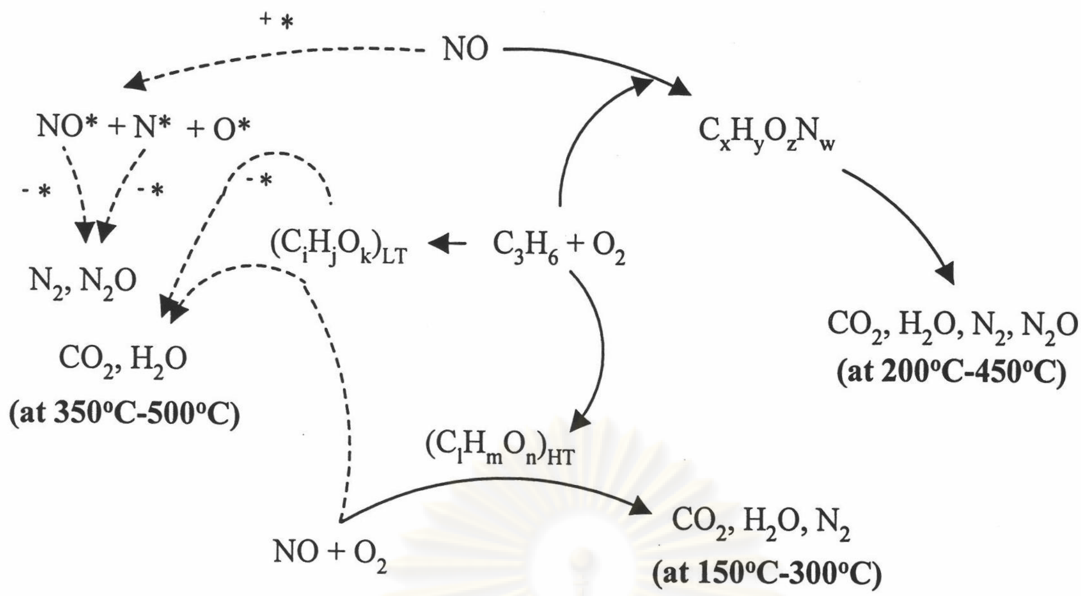

Figure 5.30 A proposed reaction mechanism scheme for the selective catalytic reduction of NO by propene under lean-burn condition over Pt/Al_2O_3 catalyst (∗ is given as the vacancy Pt sites)

5.4 Disturbance on the Function of Active Sites in the Selective Catalytic Reduction of NO by C_3H_6 under Excess Oxygen by the Addition of the Second Metal on a Pt/Al_2O_3 Catalyst

In order to understand the proposed reaction mechanism better, the additional experiments by the introduction of the second metal on a Pt/Al_2O_3 catalyst to disturb the function of active sites are proceeded in this section. This original idea is conceived from the discovery in the open literature that the main reaction mechanism in the selective catalytic reduction of NO by C_3H_6 is similar after adding any second metal on a Pt/Al_2O_3 catalyst, although each second metal can have a significant influence (either positive or negative) on the catalytic activity [139]. Hence, the different catalytic activity of modified Pt/Al_2O_3 catalysts is speculated to affect relatively the intermediate surface species. In this work, Li, Cr, Fe, Ni, Ga, Co, Sn and W are selected as the second metal.

Before the catalytic activity test and the investigation of surface species through an experimental set of three continuous steps, the characterization of modified Pt/Al_2O_3 catalysts was conducted. First, the single point BET surface area and the amount of metal active sites of modified Pt/Al_2O_3 catalyst compared with those of Pt/Al_2O_3 catalyst are shown in Table 5.3. It is obvious that all modified Pt/Al_2O_3 catalysts give less metal active sites than an unmodified Pt/Al_2O_3 catalyst. The metal active sites are particularly much lower for Pt-Li/Al_2O_3 and Pt-Sn/Al_2O_3 catalyst. While, the BET surface area fluctuates in the range from 160 m^2/g catalyst to 275 m^2/g catalyst. The XRD patterns of modified Pt/Al_2O_3 catalysts are also demonstrated in Figure 5.31. Like the former results in section 5.2, it can not be observed the different pattern of all XRD spectra and therefore they still show the characteristic peak of amorphous γ-Al_2O_3. In this work, the acidity and basicity measurements of modified Pt/Al_2O_3 catalyst are not conducted because it is proved that the acid and basic sites on Al_2O_3 are not directly involve the C_3H_6+NO+O_2 reaction on Pt-based catalyst [123-125, 134].

Table 5.3 The metal composition, the specific surface area, the metal active sites and the metal dispersion on modified Pt/Al_2O_3 catalysts

Catalyst	Pt content (%wt)	The second metal content (%wt)	The single point BET surface area (m^2/g catalyst)	Metal active sites (× 10^{19} molecule of CO/g catalyst)	Dispersion (%)
Pt/Al_2O_3	1.0	-	269	2.55	83
$Pt\text{-}Li/Al_2O_3$	1.0	1.9	160	0.93	30
$Pt\text{-}Cr/Al_2O_3$	1.1	1.8	270	2.30	68
$Pt\text{-}Fe/Al_2O_3$	0.9	1.9	238	1.98	71
$Pt\text{-}Ni/Al_2O_3$	1.0	1.9	275	2.40	78
$Pt\text{-}Ga/Al_2O_3$	1.0	2.0	227	2.12	69
$Pt\text{-}Co/Al_2O_3$	1.1	2.0	246	2.04	60
$Pt\text{-}Sn/Al_2O_3$	1.0	1.7	242	1.25	40
$Pt\text{-}W/Al_2O_3$	0.9	1.5	241	2.19	79

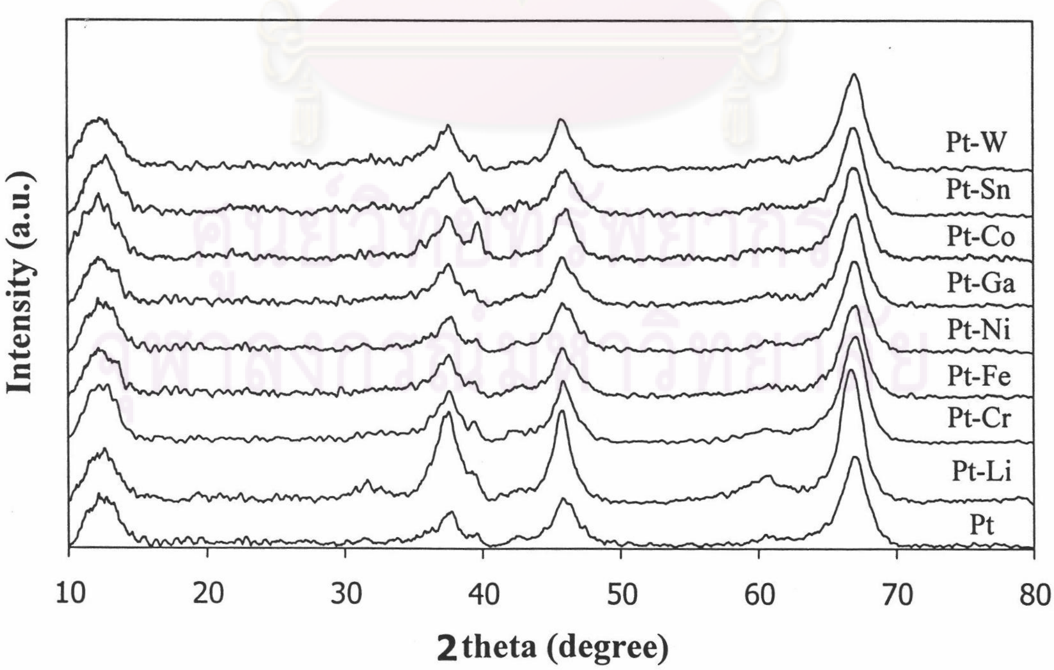

Figure 5.31 X-ray diffraction pattern of modified Pt/Al_2O_3 catalysts

The catalytic activity behavior for C_3H_6+NO+O_2 reaction on modified Pt/Al_2O_3 catalysts is examined through the temperature programmed reaction in comparison with that on monometallic Pt/Al_2O_3 catalyst. It is noted that in this section all catalysts were pre-reduced in H_2 flow and subsequently re-oxidized under 10% O_2 in He before the reaction test. Plots of C_3H_6 conversion as a function of temperature for the selective catalytic reduction of NO by C_3H_6 under excess oxygen on these catalysts are given in Figures 5.32, 5.34, 5.36 and 5.38. While Figures 5.33, 5.35, 5.37 and 5.39 show total NO conversions (to N_2 and N_2O) obtained to be connected with C_3H_6 conversion in the same reaction.

It is obvious that the addition of the second metal, with the exception of Li, over monometallic Pt/Al_2O_3 catalyst hardly affects the behavior of catalytic activity, viz., the C_3H_6 light-off temperature, the maximum NO conversion and the temperature of maximum NO conversion for such reaction. Pt-Li/Al_2O_3 shows the best catalytic activity among the selected modified Pt/Al_2O_3 catalysts. It is important to realize that a large amount of N_2O is detected at all temperature ranges where NO conversions appear for all catalysts. The N_2O selectivity of each catalyst at temperature of its maximum NO conversion is approximately in the range of 60-75%. Similar N_2O selectivities of the modified catalysts and unmodified Pt/Al_2O_3 correspond with the earlier work [139]. However, the narrow temperature window of their catalytic activities for all catalysts becomes an essential obstruction in the consideration of the intrinsic activity in detail. To elucidate the influence of the second metal on the catalytic activity better, the turnover numbers (TONs) of C_3H_6 and NO conversions at 225°C are obtained as given in Table 5.4.

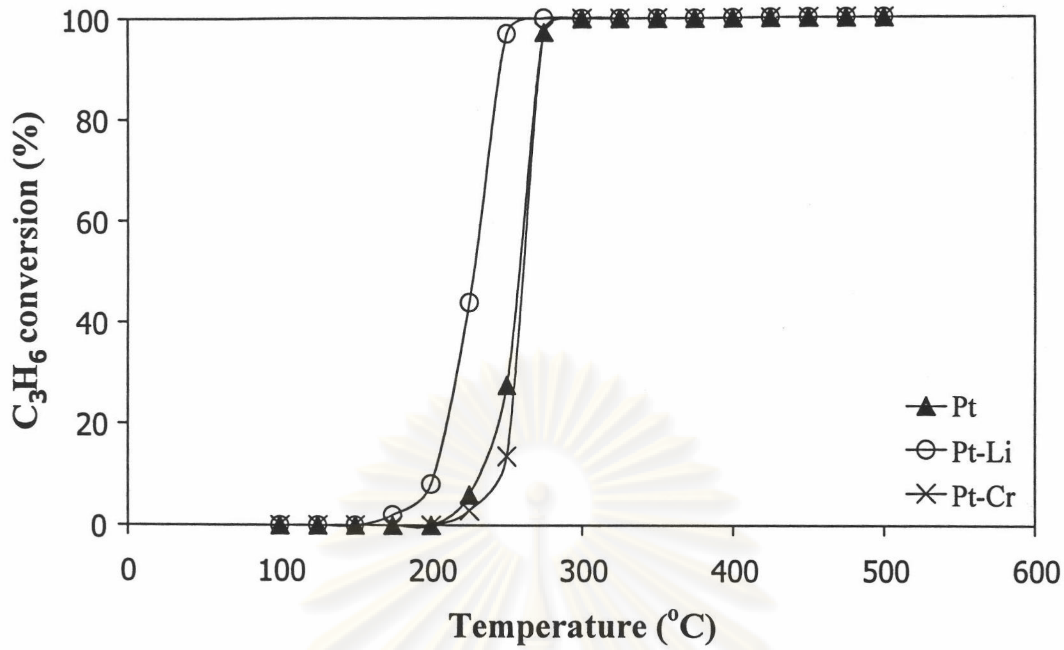

Figure 5.32 The effect of Li or Cr on C_3H_6 conversion on Pt/Al_2O_3 catalyst for the selective catalytic reduction of NO by C_3H_6 under excess oxygen

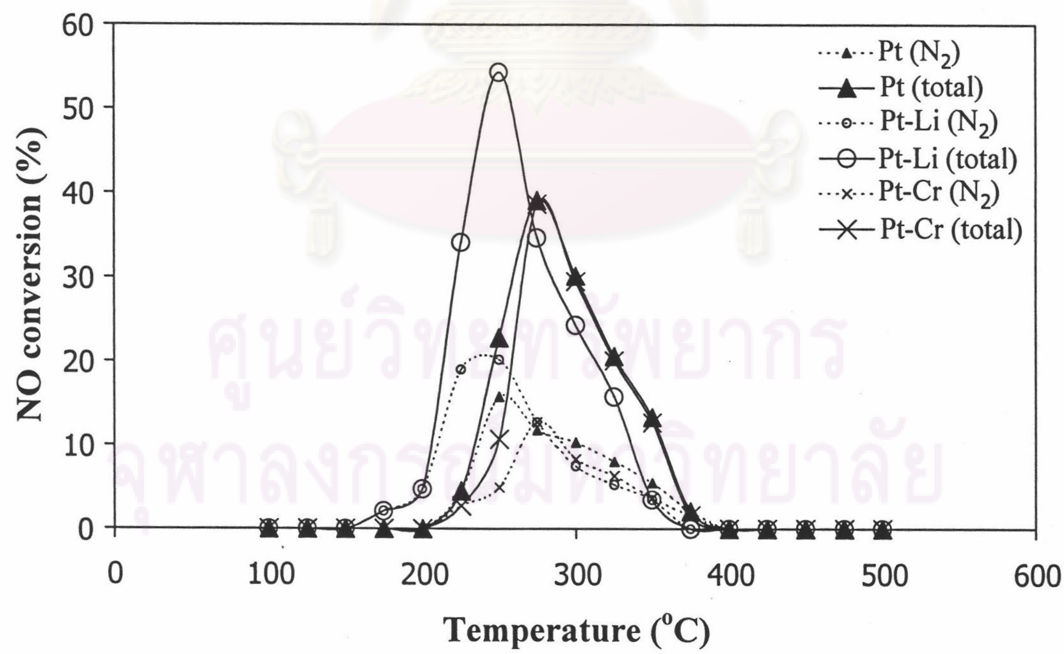

Figure 5.33 The effect of Li or Cr on NO conversion to N_2 and N_2O on Pt/Al_2O_3 catalyst for the selective catalytic reduction of NO by C_3H_6 under excess oxygen

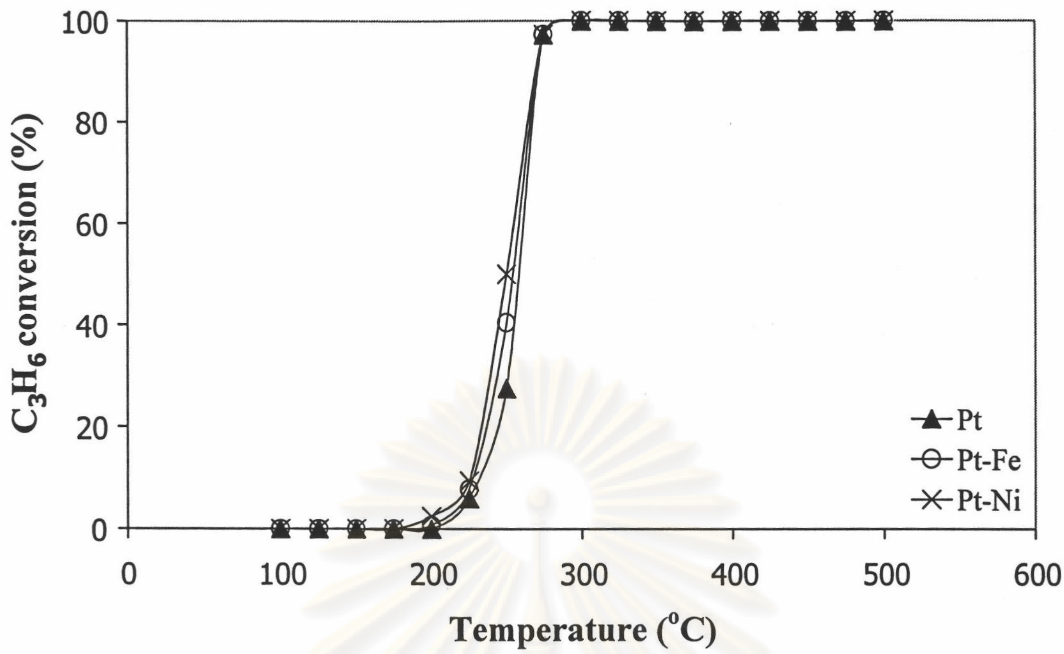

Figure 5.34 The effect of Fe or Ni on C_3H_6 conversion on Pt/Al_2O_3 catalyst for the selective catalytic reduction of NO by C_3H_6 under excess oxygen

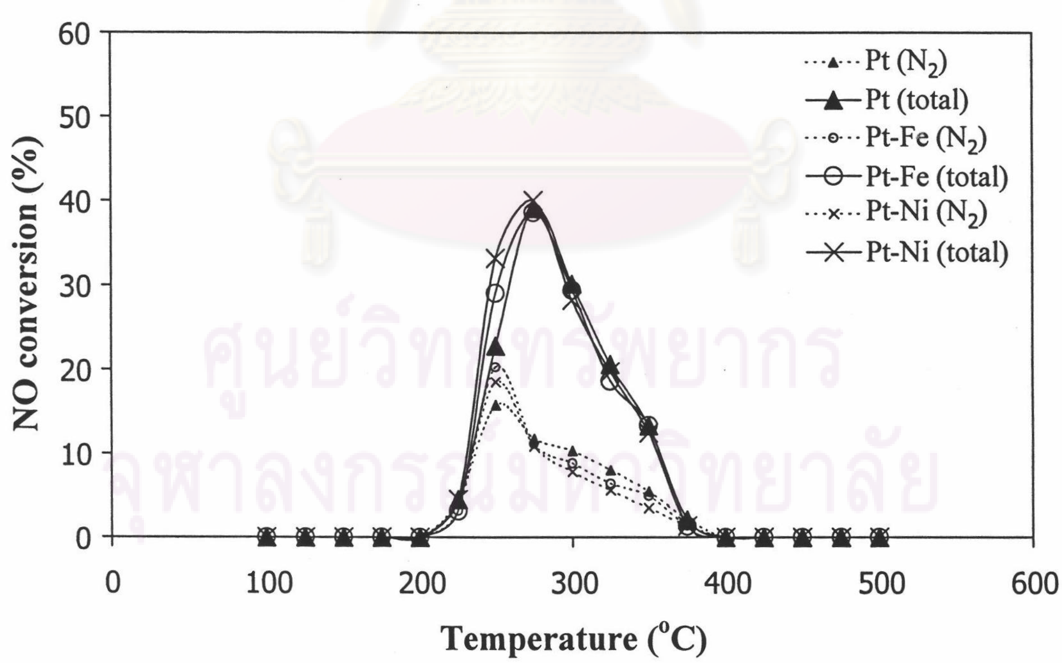

Figure 5.35 The effect of Fe or Ni on NO conversion to N_2 and N_2O on Pt/Al_2O_3 catalyst for the selective catalytic reduction of NO by C_3H_6 under excess oxygen

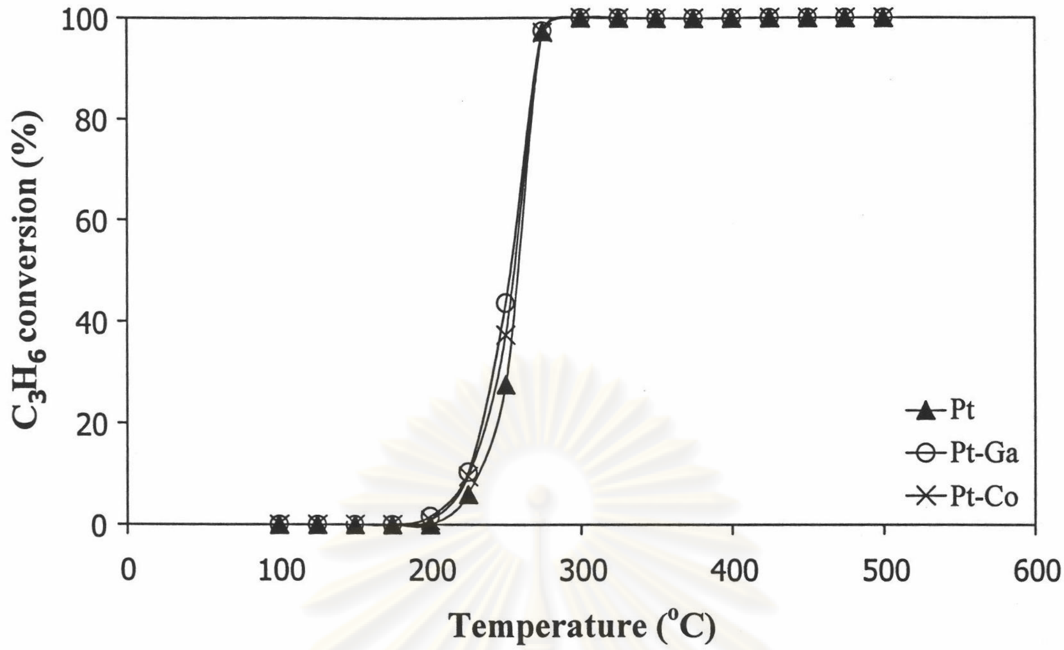

Figure 5.36 The effect of Ga or Co on C_3H_6 conversion on Pt/Al_2O_3 catalyst for the selective catalytic reduction of NO by C_3H_6 under excess oxygen

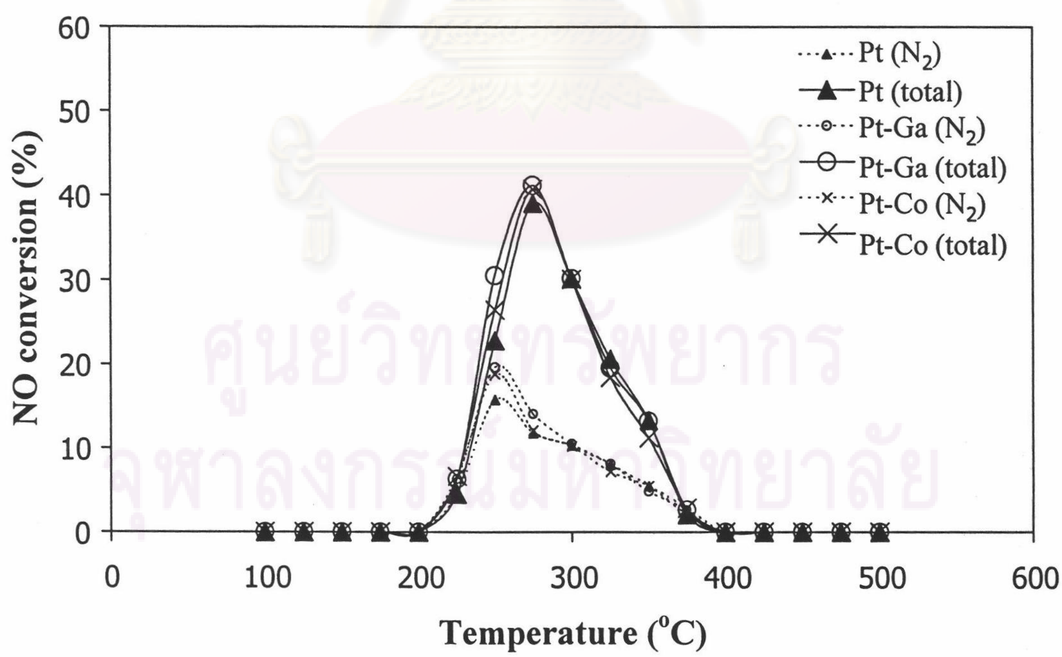

Figure 5.37 The effect of Ga or Co on NO conversion to N_2 and N_2O on Pt/Al_2O_3 catalyst for the selective catalytic reduction of NO by C_3H_6 under excess oxygen

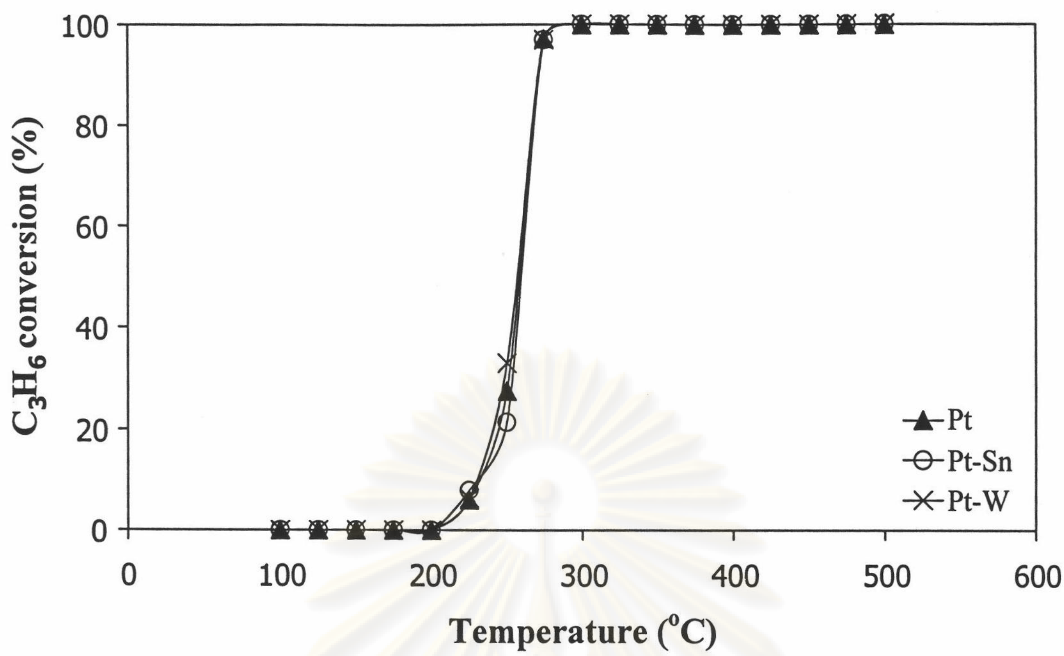

Figure 5.38 The effect of Sn or W on C_3H_6 conversion on Pt/Al_2O_3 catalyst for the selective catalytic reduction of NO by C_3H_6 under excess oxygen

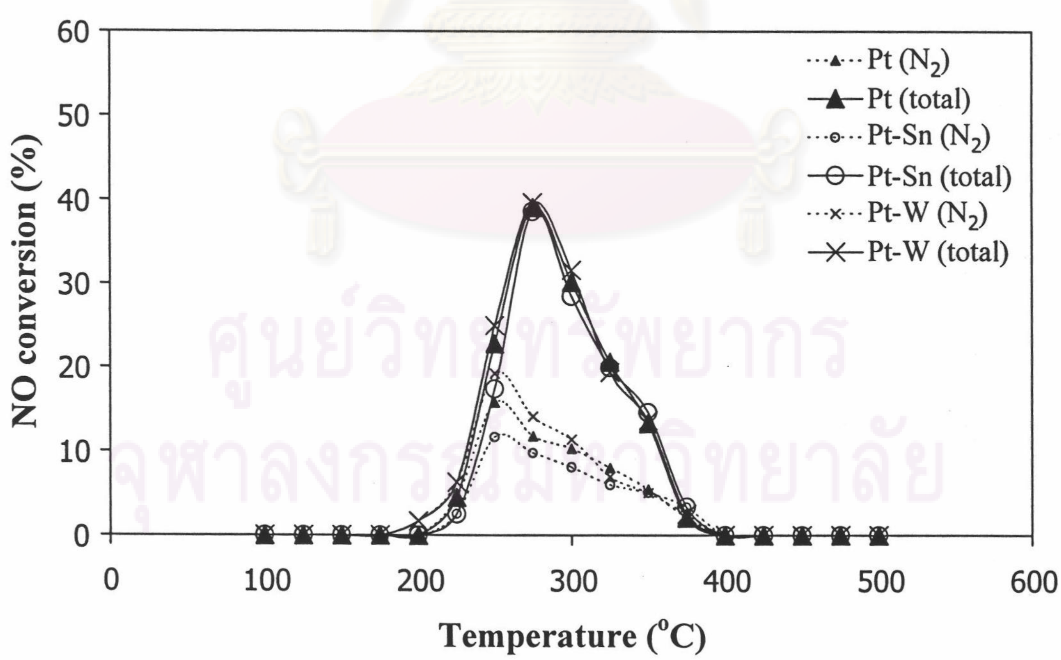

Figure 5.39 The effect of Sn or W on NO conversion to N_2 and N_2O on Pt/Al_2O_3 catalyst for the selective catalytic reduction of NO by C_3H_6 under excess oxygen

Table 5.4 The turnover number of C_3H_6 and NO conversions at 225°C

Catalyst	TON of C_3H_6 ($\times10^{-2}$/s)	TON of NO ($\times10^{-2}$/s)
Pt/Al_2O_3	0.90	0.47
$Pt\text{-}Li/Al_2O_3$	3.92	2.03
$Pt\text{-}Cr/Al_2O_3$	0.37	0.15
$Pt\text{-}Fe/Al_2O_3$	1.50	0.74
$Pt\text{-}Ni/Al_2O_3$	1.37	0.97
$Pt\text{-}Ga/Al_2O_3$	1.83	1.17
$Pt\text{-}Co/Al_2O_3$	1.15	0.72
$Pt\text{-}Sn/Al_2O_3$	1.33	0.77
$Pt\text{-}W/Al_2O_3$	0.86	0.49

As seen in Figures 5.32-5.39 and Table 5.4, it is clear that although the similarity in catalytic activity behavior towards the temperature programmed reaction of the modified catalysts and unmodified Pt/Al_2O_3 catalyst is pronounced, the different TONs of these catalysts definitely indicate the disturbance in some function of active sites over Pt/Al_2O_3 by the second metal. It is significantly remarked that TONs of both C_3H_6 and NO conversions of $Pt\text{-}Li/Al_2O_3$ catalyst are about four times more than those of Pt/Al_2O_3 catalyst corresponding with the results from temperature programmed reaction. On the negative side, $Pt\text{-}Cr/Al_2O_3$ catalyst provides the lowest TONs of C_3H_6 and NO conversions both being approximately three times less than those of monometallic Pt catalyst. From the different TONs of these catalysts, it is interesting to seek the nature of surface species on each modified catalyst compared with that on unmodified catalyst because these surface species may play an important role on the determination of the reaction mechanism pathway as discussed in the above section. The presence of the second metal on Pt/Al_2O_3 can intrinsically result in the difference of TPD pattern obtained by the second step in an experimental set of three continuous steps as shown in Figures 5.41-5.48. It is noted that the TPD profile of Pt/Al_2O_3 catalyst shown previously in Figure 5.16 is again exhibited in Figure 5.40 to be easy in the comparative observation.

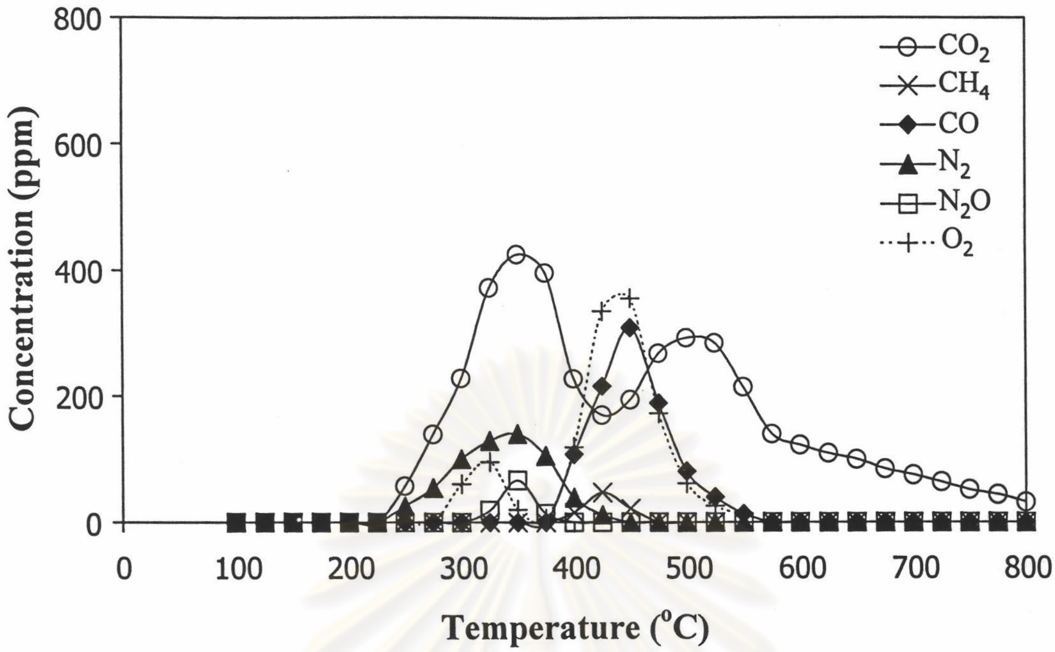

Figure 5.40 The temperature programmed desorption profiles of Pt/Al_2O_3 catalyst after dosing 1000 ppm C_3H_6 + 1000 ppm NO + 5% O_2 at 225°C for 2 h

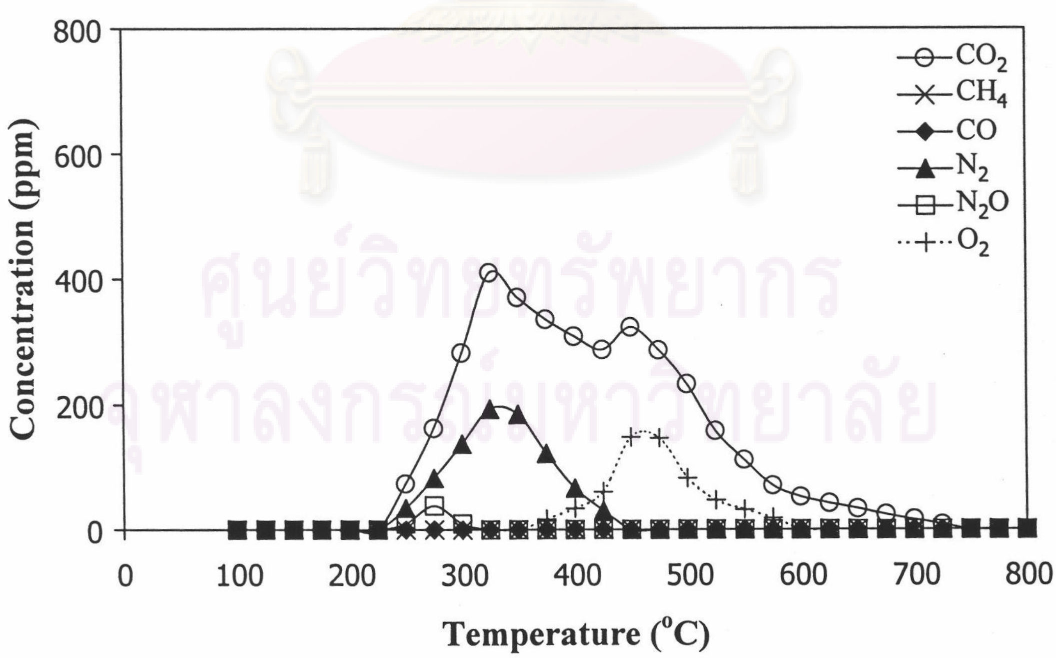

Figure 5.41 The temperature programmed desorption profiles of $Pt\text{-}Li/Al_2O_3$ catalyst after dosing 1000 ppm C_3H_6 + 1000 ppm NO + 5% O_2 at 225°C for 2 h

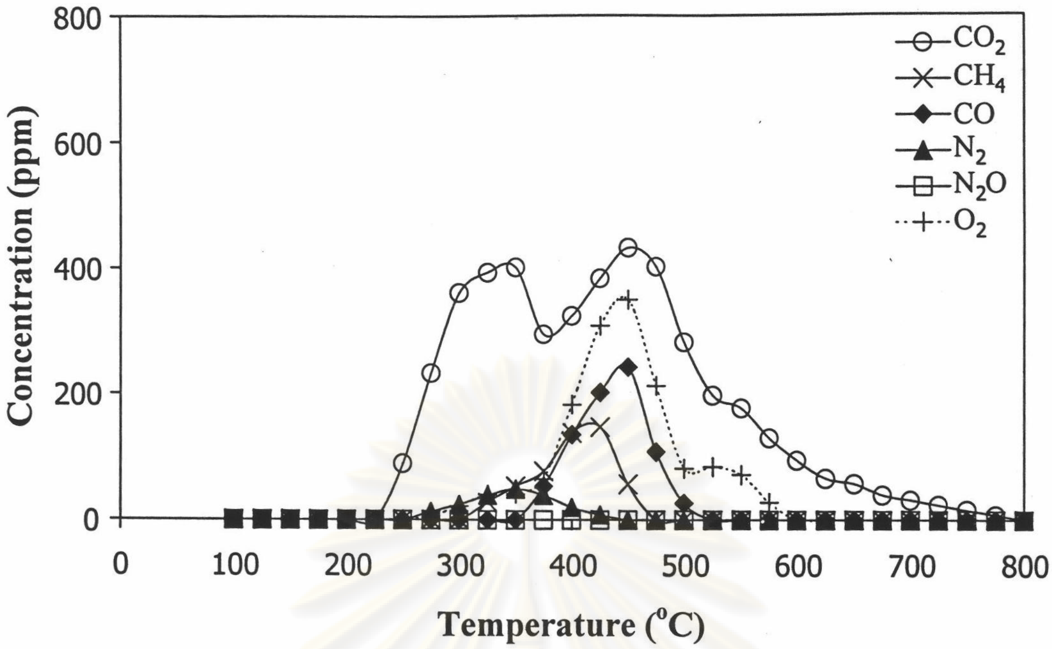

Figure 5.42 The temperature programmed desorption profiles of Pt-Cr/Al_2O_3 catalyst after dosing 1000 ppm C_3H_6 + 1000 ppm NO + 5% O_2 at 225°C for 2 h

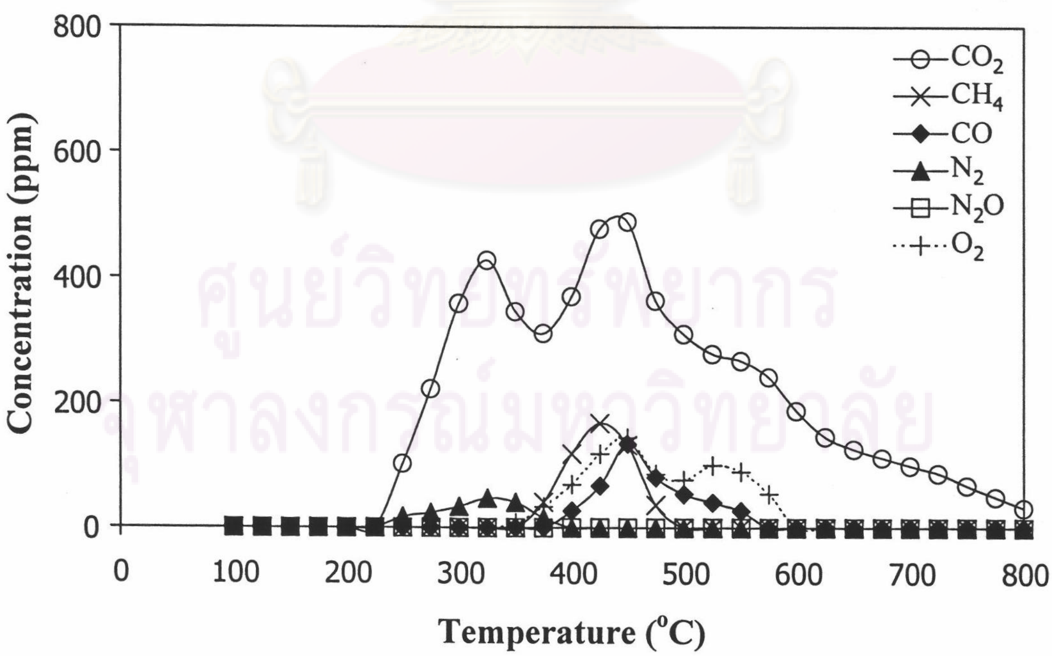

Figure 5.43 The temperature programmed desorption profiles of Pt-Fe/Al_2O_3 catalyst after dosing 1000 ppm C_3H_6 + 1000 ppm NO + 5% O_2 at 225°C for 2 h

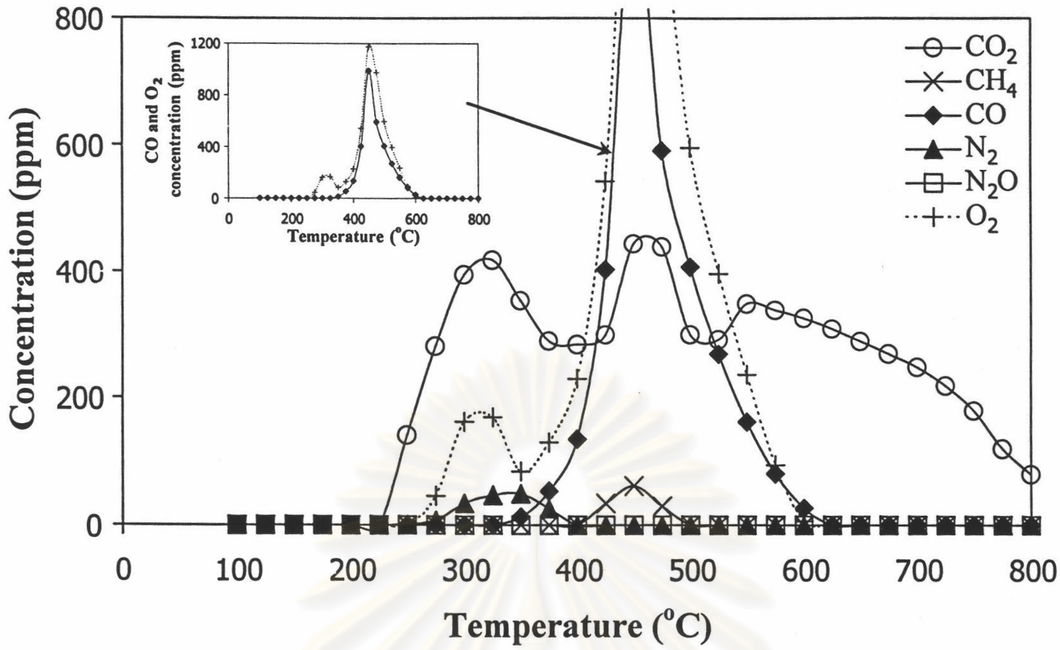

Figure 5.44 The temperature programmed desorption profiles of Pt-Ni/Al_2O_3 catalyst after dosing 1000 ppm C_3H_6 + 1000 ppm NO + 5% O_2 at 225°C for 2 h

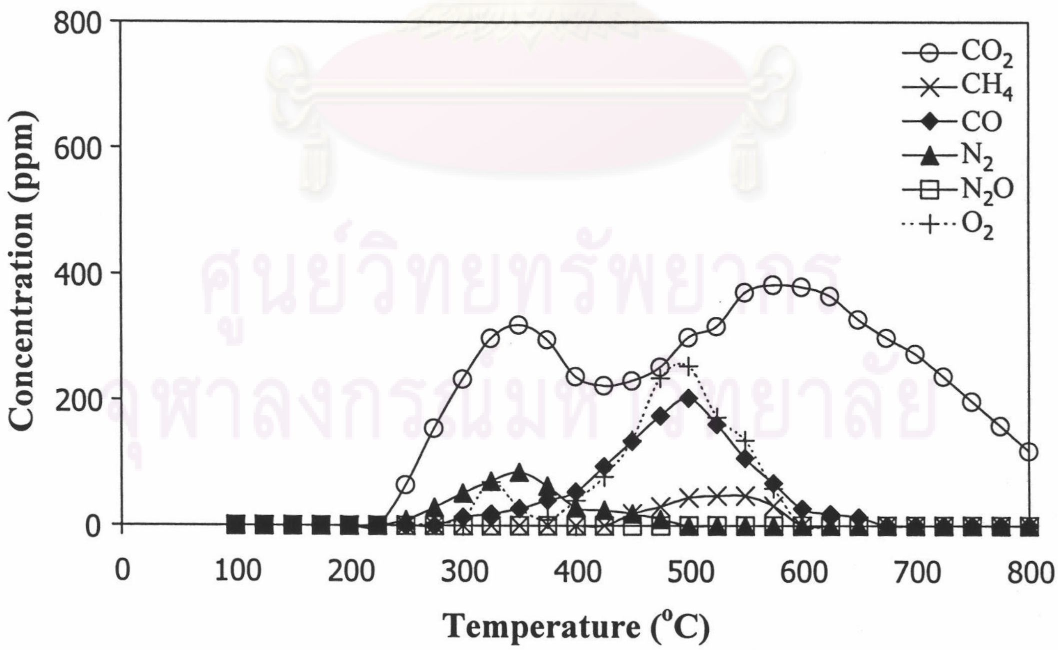

Figure 5.45 The temperature programmed desorption profiles of Pt-Ga/Al_2O_3 catalyst after dosing 1000 ppm C_3H_6 + 1000 ppm NO + 5% O_2 at 225°C for 2 h

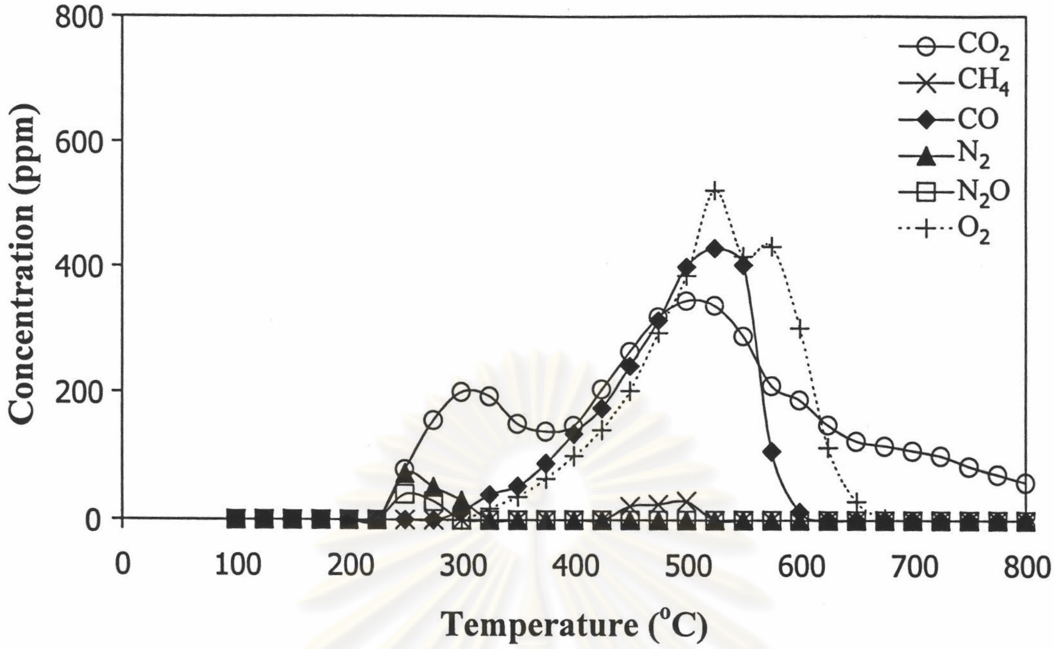

Figure 5.46 The temperature programmed desorption profiles of Pt-Co/Al_2O_3 catalyst after dosing 1000 ppm C_3H_6 + 1000 ppm NO + 5% O_2 at 225°C for 2 h

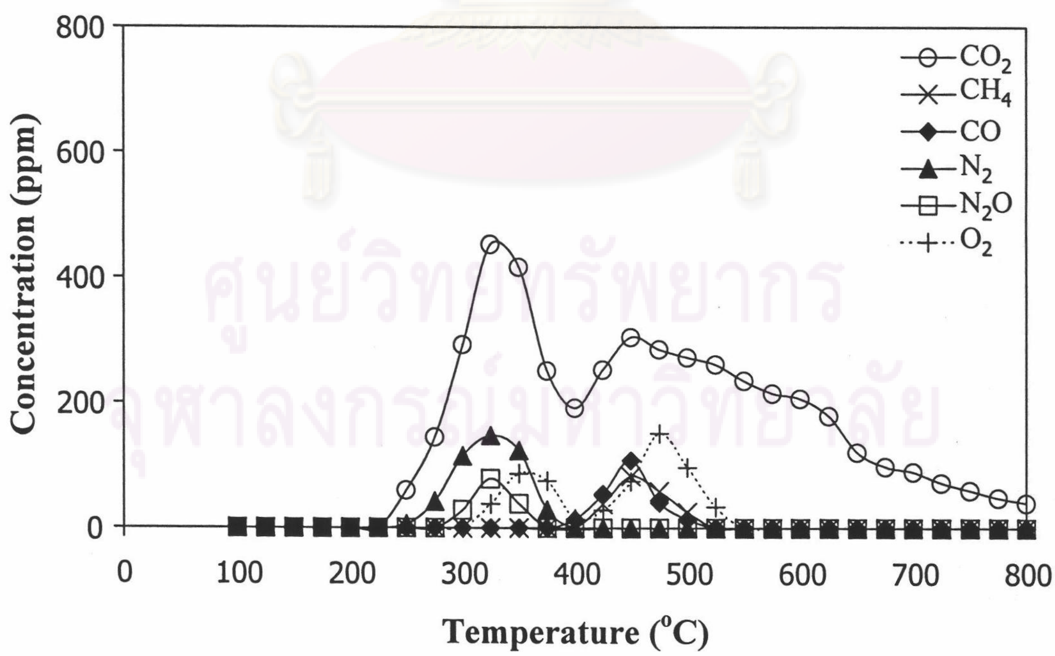

Figure 5.47 The temperature programmed desorption profiles of Pt-Sn/Al_2O_3 catalyst after dosing 1000 ppm C_3H_6 + 1000 ppm NO + 5% O_2 at 225°C for 2 h

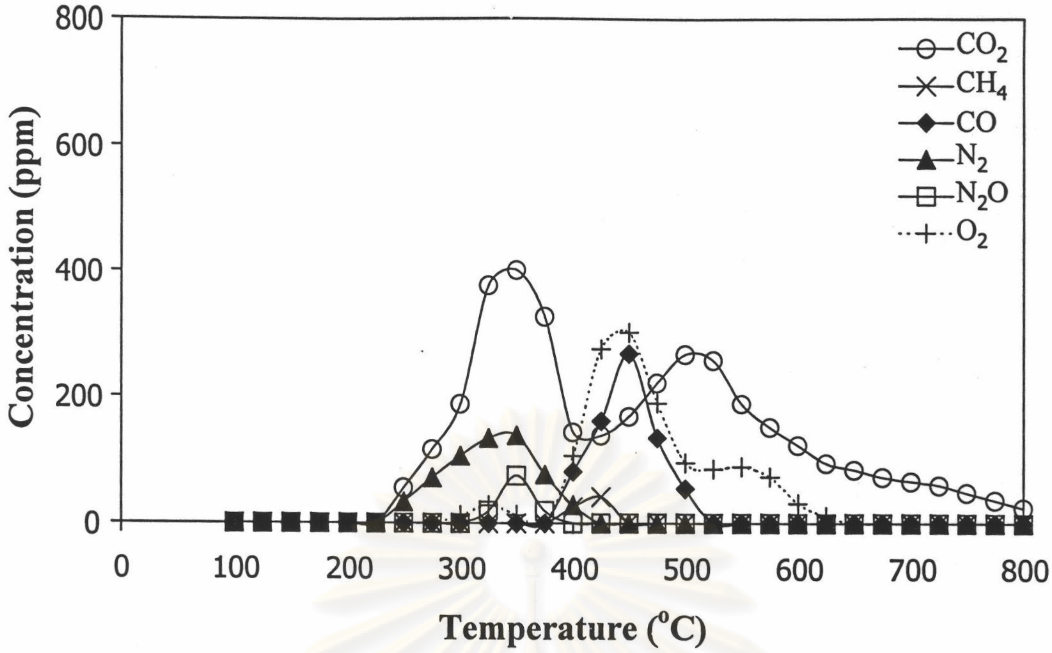

Figure 5.48 The temperature programmed desorption profiles of Pt-W/Al_2O_3 catalyst after dosing 1000 ppm C_3H_6 + 1000 ppm NO + 5% O_2 at 225°C for 2 h

It is obvious that the nature of surface species on Pt/Al_2O_3 catalyst modified by any second metal is different from that on the monometallic Pt/Al_2O_3 catalyst; however, the similar composition of surface species involving C, H, O and N atoms, which are released in form of CO_2, CH_4, CO, N_2, N_2O and O_2, are observed. For all modified catalysts, the observation of carbon containing product (CO_2 and CO) peaks at the same or small shifted position where $C_xH_yO_zN_w$, $(C_iH_jO_k)_{LT}$, and $(C_lH_mO_n)_{HT}$ species is identified in case of Pt/Al_2O_3 catalyst indicates that three types of surface species can be produced on all catalytic system tested in this work. Nevertheless, the disappearance of carbon dioxide peak at high temperature (525°C) on Pt-Li/Al_2O_3 catalyst shows the absence of $(C_lH_mO_n)_{HT}$ species on this catalyst. Pt-W/Al_2O_3 giving the TONs of C_3H_6 and NO conversions close to Pt/Al_2O_3 seems to provide rather similar characteristic of surface species. However, it should be noted that there is an additional O_2 peak at high temperature (550°C) after the addition of W. In case of Pt-Sn/Al_2O_3, the outlet gases released by the decomposition of $C_xH_yO_zN_w$ species show the same behavior with those of Pt/Al_2O_3. Interestingly, an additional CO_2 peak and a lower amount of the outlet CO and O_2 at moderate temperature (450°C) and a broader CO_2 peak at high temperature (525°C) indicate a little change in the nature of

$(C_iH_jO_k)_{LT}$, and $(C_lH_mO_n)_{HT}$ species on the catalyst surface. The nature of surface species on Pt-Fe/Al_2O_3, Pt-Cr/Al_2O_3 and Pt-Ni/Al_2O_3 is rather similar. Comparing to the surface species on Pt/Al_2O_3, an additional CO_2 peak at moderate temperature (450°C), the tiny shift to higher temperature of a CO_2 peak from $(C_lH_mO_n)_{HT}$ species being coincident with the appearance of O_2 peak at the same temperature (525°C) and the disappearance of N_2O peak from $C_xH_yO_zN_w$ species are clearly observed on three catalysts. It is remarked that a plenty amount of $(C_iH_jO_k)_{LT}$ species is produced on Pt-Ni/Al_2O_3 catalyst due to a large production of CO and O_2 at 450°C. The nature of surface species on Pt-Ga/Al_2O_3 and Pt-Co/Al_2O_3 are rather a unique behavior compared with that of Pt/Al_2O_3. $(C_iH_jO_k)_{LT}$, and $(C_lH_mO_n)_{HT}$ species observed on both catalysts decompose themselves at higher temperature, which give the carbon dioxide peaks at 500°C and 600°C. The shift of carbon monoxide and oxygen peak addressed as $(C_iH_jO_k)_{LT}$ species from 450°C to 500°C confirms this speculation.

From the above-proposed mechanism in section 5.3.4, the reactivity to NO+O_2 of $(C_lH_mO_n)_{HT}$ species and the themselves-decomposition of $C_xH_yO_zN_w$ species are speculated to be the significant cooperative mechanism pathway for the SCR of NO by C_3H_6 on Pt/Al_2O_3 in the operating temperature range (200°C to 400°C) and $C_xH_yO_zN_w$ and $(C_lH_mO_n)_{HT}$ species should be therefore speculated as the key intermediate species at 225°C. Hence, the amount of $C_xH_yO_zN_w$ and $(C_lH_mO_n)_{HT}$ species in TPD profile of each catalyst is carefully considered. It is noted that the amount of $(C_iH_jO_k)_{LT}$ species is absolutely negligible because they decompose themselves at high temperature and are inactive with the reactant at low temperature. The amount of C atoms obtained by the deconvolution of carbon dioxide profile represents the amount of $C_xH_yO_zN_w$ and $(C_lH_mO_n)_{HT}$ species, which an example of calculation is shown in Appendix G. It appears that the steady state C_3H_6 and NO conversions obtained from the first step in an experimental set of three continuous steps is not related simply to the amount of $C_xH_yO_zN_w$ species whereas C_3H_6 and NO conversions is surprisingly dependent on the amount of $(C_lH_mO_n)_{HT}$ species as shown in Figures 5.49 and 5.50, respectively. Therefore, $(C_lH_mO_n)_{HT}$ species are presumably important in the selective catalytic reduction of NO by C_3H_6 under oxygen excess over Pt-based catalyst at low temperature whereas the decomposition of $C_xH_yO_zN_w$ species occurs only to a minor extent.

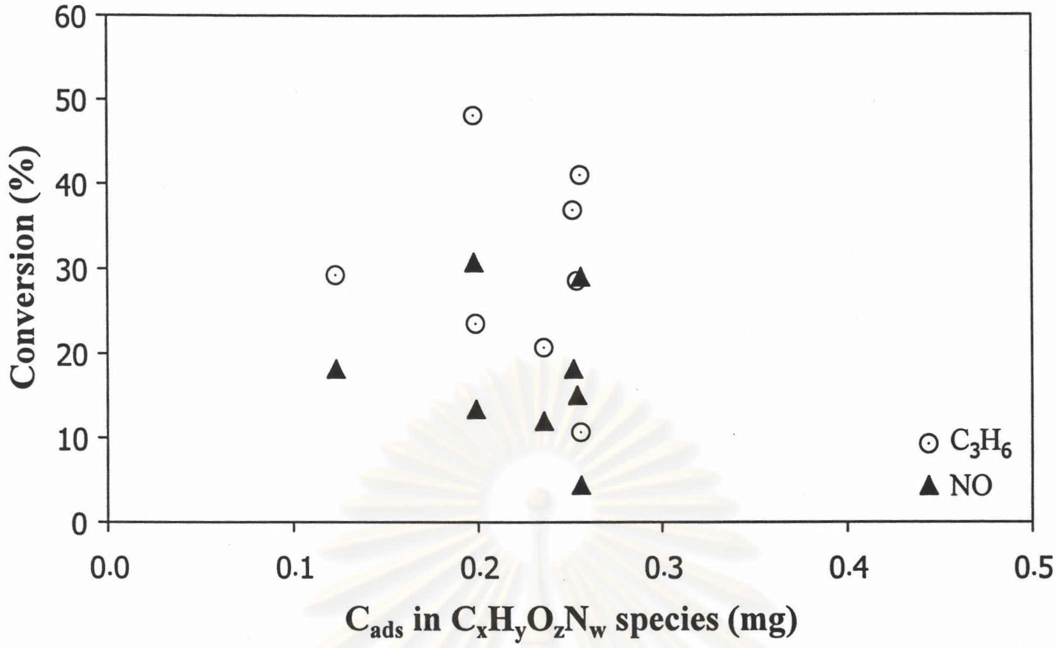

Figure 5.49 The relationship between the amount of $C_xH_yO_zN_w$ species and C_3H_6 and NO conversions obtained during the first step in an experimental set of three continuous steps at 225°C for 2 h

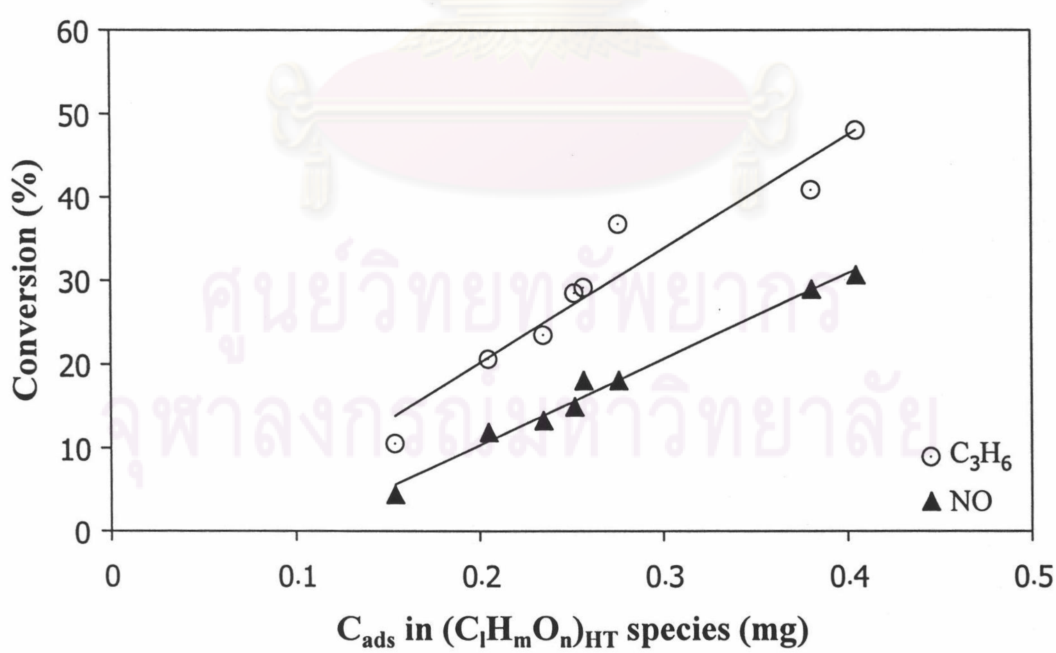

Figure 5.50 The relationship between the amount of $(C_lH_mO_n)_{HT}$ species and C_3H_6 and NO conversions obtained during the first step in an experimental set of three continuous steps at 225°C for 2 h

Another evidence indicating that $(C_lH_mO_n)_{HT}$ species play an important role on the reaction mechanism at low temperature is the catalytic activity test towards SO_2 cycle of Pt-Li/Al_2O_3 catalyst. The above results in section 5.3.3 show that the introduction of SO_2 into the feed stream results in the loss of much amount of $C_xH_yO_zN_w$ species and the decrease of $(C_lH_mO_n)_{HT}$ species coincident with the drop of C_3H_6 and NO conversions. Thus, if the SO_2 was switch into the reactant on Pt-Li/Al_2O_3 catalyst, the C_3H_6+NO+O_2 reaction should be strongly inhibited due to no $(C_lH_mO_n)_{HT}$ species contributing the production of CO_2 and N_2 products on this catalyst. The effect of adding 500 ppm of SO_2 to reaction feed as a function of time for Pt-Li/Al_2O_3 catalyst is shown in Figure 5.51. It is clear that C_3H_6 and NO conversions do not only decrease after introducing SO_2 into the feed but also have no return to the previous steady state. It is envisaged that the reaction mechanism pathway of Pt-Li/Al_2O_3 catalyst is different from that of others. The decomposition of $C_xH_yO_zN_w$ species becomes a dominant mechanism and SO_2 strongly inhibits this pathway.

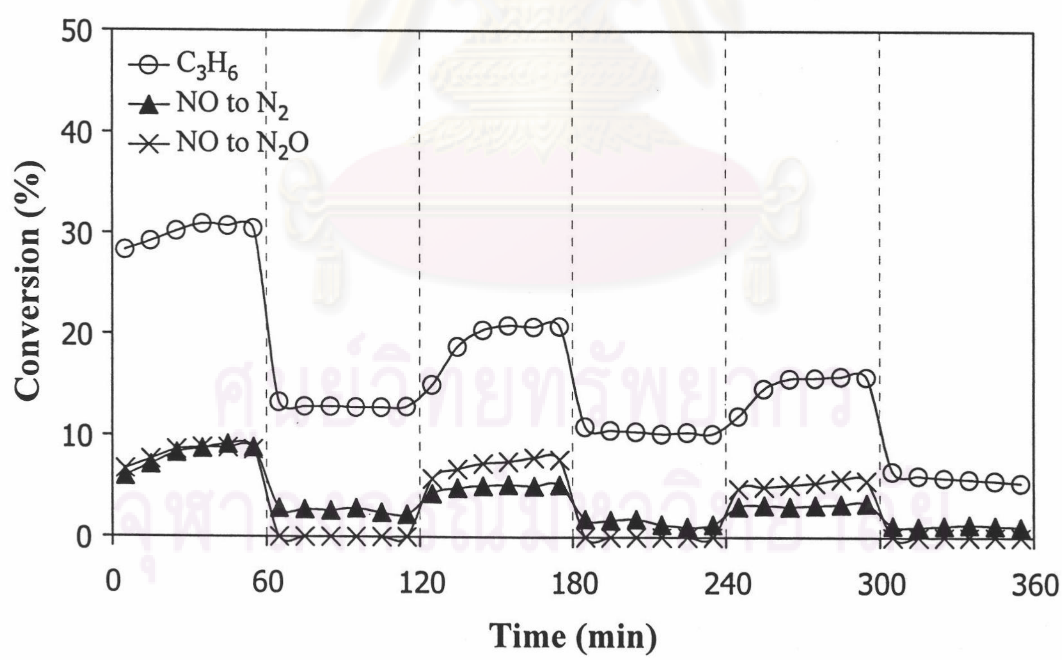

Figure 5.51 The effect of switching 500 ppm SO_2 into and out of the feed stream on the C_3H_6+NO+O_2 reaction over Pt-Li/Al_2O_3 catalyst at 225°C as a function of time

5.5 Mechanistic Studies in the Selective Catalytic Reduction of NO under Excess Oxygen on Pt-based Catalysts using C_3H_8 as a Reductant instead of C_3H_6

The success in the prediction of reaction mechanism for the selective catalytic reduction of NO by C_3H_6 under excess oxygen on Pt/Al_2O_3 catalyst leads us to the expansion of the investigation of surface species by this procedure into the other reactions. The selective catalytic reduction of NO by C_3H_8 under excess oxygen is chosen due to the lack of the mechanistic studies. A little amount of the previously published papers about the use of C_3H_8 as a reductant are due to a much low activity for NO reduction, perhaps no activity [159]. However, in real diesel engine the paraffinic hydrocarbons are mixed with the other hydrocarbon substances; therefore, the profound understanding in the reaction mechanism may assist to elevate the catalytic development in this field.

Like the selective catalytic reduction of NO by C_3H_6 under excess oxygen, two sets of Pt/Al_2O_3 catalyst on which the different surface oxygen was first prepared by the two different pretreatments were tested by the catalytic activity measurement toward temperature programmed reaction. Figure 5.52 shows the comparison of temperature programmed reaction profile involving C_3H_8 and NO conversions versus the elevated temperature between Pt_{ox}/Al_2O_3 and Pt_{red}/Al_2O_3 catalysts. Both of catalysts show the same profile of C_3H_8 conversion while the maximum peak of NO conversion for Pt_{ox}/Al_2O_3 catalyst shift to higher temperature compared with that for Pt_{red}/Al_2O_3 catalyst. The NO reduction reaches a sharp maximum of approximately 14% at 425°C and 17% at 450°C for Pt_{red}/Al_2O_3 and Pt_{ox}/Al_2O_3 catalysts, respectively. Unlike the catalytic activity behavior for the reaction with C_3H_6, the onset of NO reduction and the peak in the NO conversion are not related to the C_3H_8 oxidation. Although conversions of C_3H_8 and NO begin at the same temperature and raise together, the NO reduction reaches a maximum value before the C_3H_8 oxidation is complete. This result indicates that the C_3H_8 activation on Pt-based catalyst is independent on the feature of surface oxygen. It is significantly noted that both catalysts do not absolutely produce N_2O.

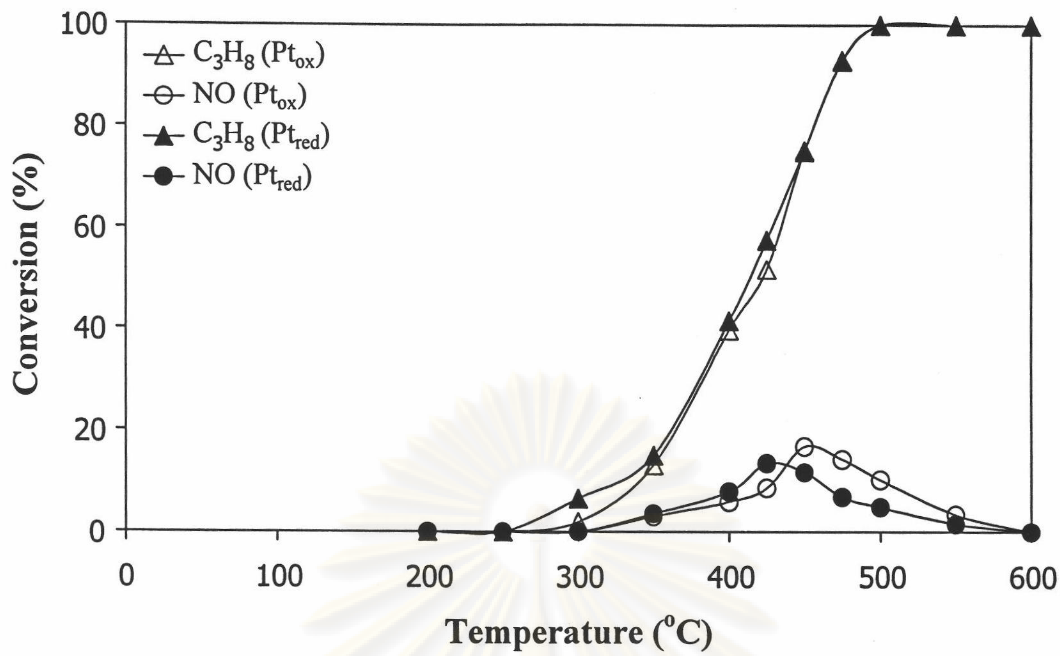

Figure 5.52 The temperature programmed reaction profiles of Pt_{ox}/Al_2O_3 and Pt_{red}/Al_2O_3 catalysts for the selective catalytic reduction of NO by C_3H_8 under excess oxygen

The effect of the presence of NO on the C_3H_8 oxidation activity of Pt_{ox}/Al_2O_3 and Pt_{red}/Al_2O_3 catalysts was also examined. With only Pt_{red}/Al_2O_3 catalysts the presence of NO slightly retards the activation of C_3H_8 by 25°C, as can be seen in Figure 5.53. This result indicates C_3H_8 reacting favorably with oxygen even in the presence of NO. The high surface coverage of oxygen as mentioned in the previous work [155] may be possibly rational.

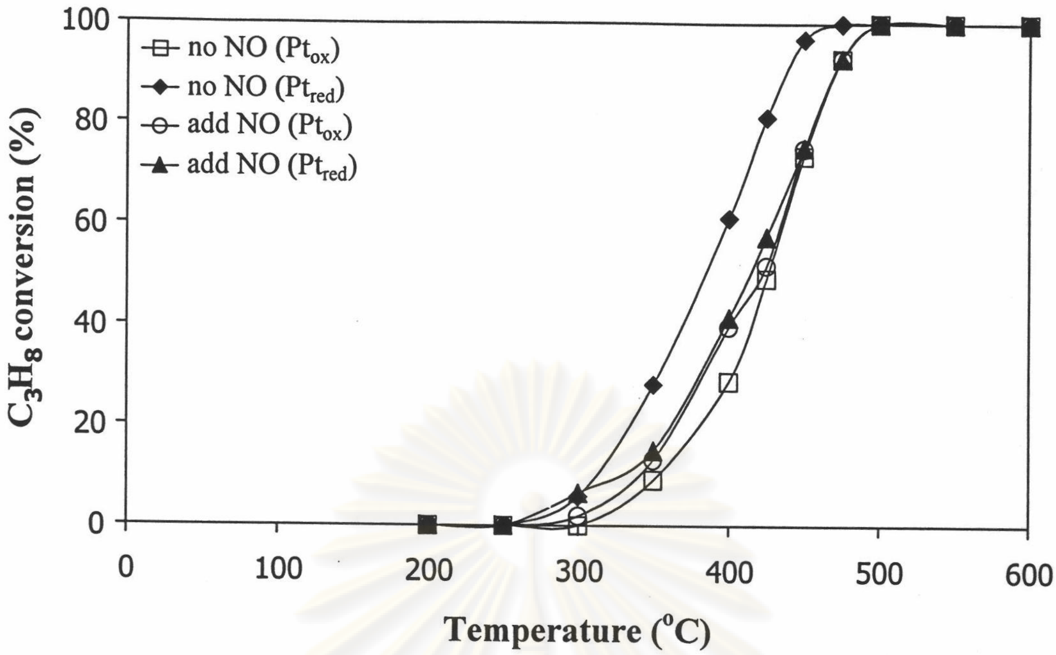

Figure 5.53 Effect of the presence of NO on C_3H_8 oxidation activity on Pt_{ox}/Al_2O_3 and Pt_{red}/Al_2O_3 catalysts

Due to the suggestion in the literature that the adsorbed propyl species reaction step for the NO reduction by C_3H_8 were rapid, a less coverage of C_3H_8-derived species would build up on the catalyst surface [155]. Hence, the investigation of the surface species over Pt_{red}/Al_2O_3 is first conducted to ensure that the amount of surface species is enough for the consideration in detail. After dosing the gas mixture of C_3H_8+NO+O_2 at 350°C for 2 h, the temperature programmed desorption step was conducted. Figure 5.50 illustrates the traces of carbon dioxide during TPD step. It is significantly remarked that only two product gases containing carbon dioxide and nitrogen was detected during TPD step. However, the amount of nitrogen releasing gas is very small, ca. 20 ppm of maximum value, and therefore it is neglected. While the amount of outlet gases by TPO step is still extremely small, like the reaction with C_3H_6. Considering the profile of carbon dioxide, there is a peak at 425°C. These surface species behave similar to $(C_iH_jO_k)_{LT}$ species detected in the C_3H_6+NO+O_2 system because they is slightly active with O_2 and NO+O_2 from the reactivity test as also shown in Figure 5.54.

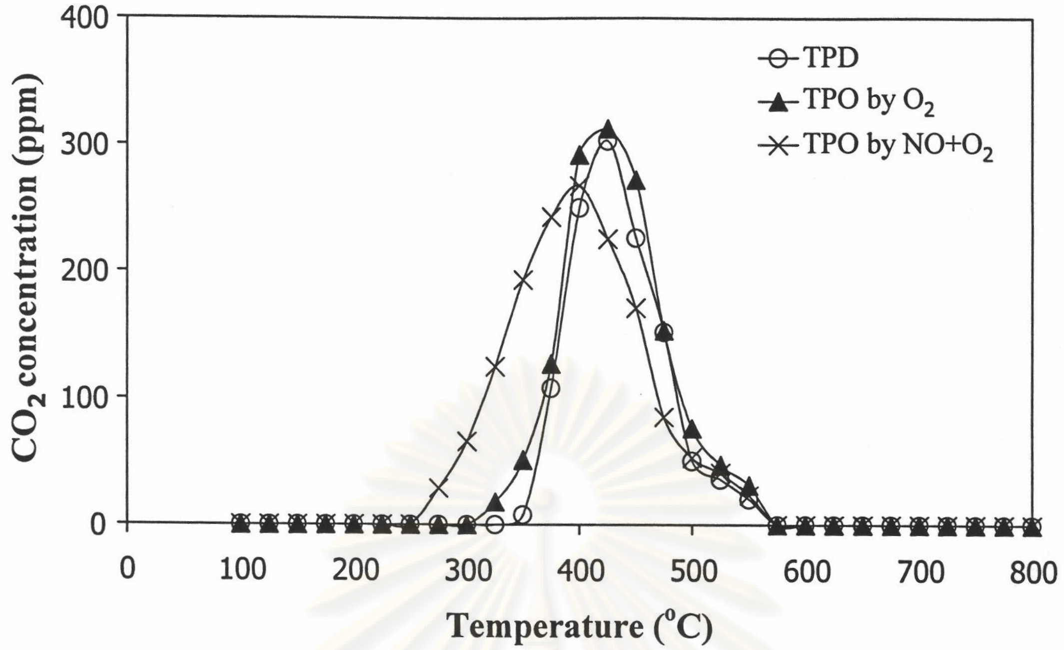

Figure 5.54 The carbon monoxide profiles from TPD, TPO by 1% O_2 and TPO by 1000 ppm NO + 1% O_2 of Pt_{red}/Al_2O_3 after dosing 1000 ppm C_3H_6 + 1000 ppm NO + 5% O_2 at 225°C for 2 h

Since the results that the NO+O_2 mixture reacts more easily with $(C_iH_jO_k)_{LT}$ species than only O_2 contrast with the inhibition of C_3H_8 oxidation by the presence of NO, which is observed in the catalytic activity test, it is envisaged that these surface species should be the spectator species or the minor intermediate species. Therefore, the investigation of surface species by this technique can not apply with the selective catalytic reduction of NO by C_3H_8 under excess oxygen on Pt/Al_2O_3 catalyst. However, in order to confirm that $(C_iH_jO_k)_{LT}$ species are unaffected conversions of C_3H_8 and NO, the catalytic activity behavior of the second metal-modified Pt/Al_2O_3 catalyst is considered coupling with the nature of surface species on these catalysts. Figures 5.55 and 5.57 show plots of C_3H_6 conversion as a function of temperature for the selective catalytic reduction of NO by C_3H_8 under excess oxygen on modified catalysts. While Figures 5.56 and 5.58 demonstrate the NO conversions to N_2 obtained to be connected with C_3H_6 conversion in the same reaction.

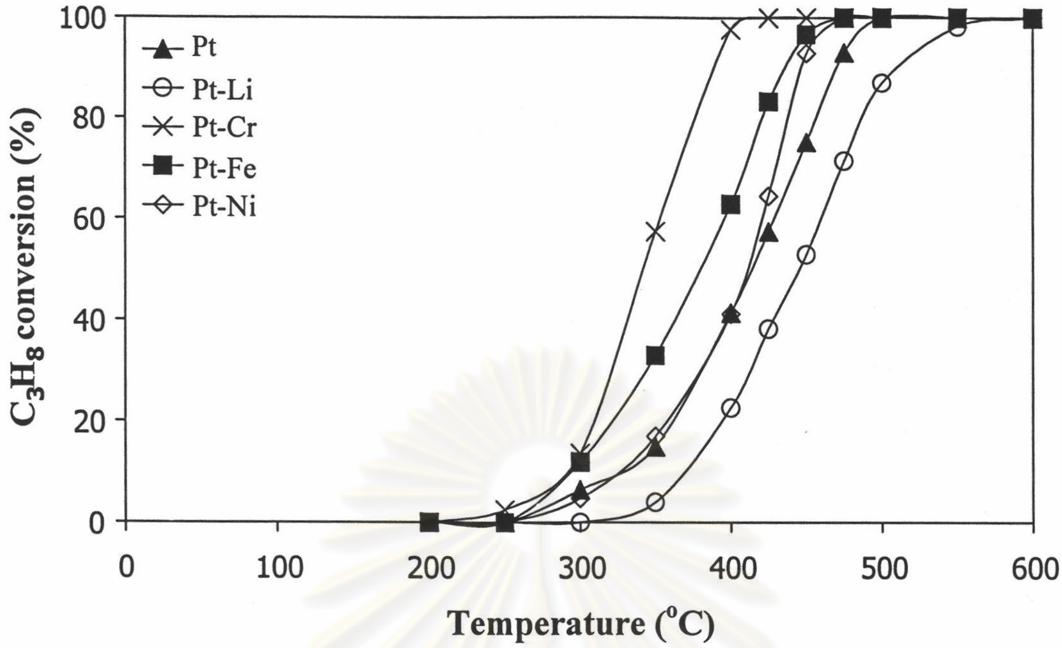

Figure 5.55 The effect of Li, Cr, Fe or Ni on C_3H_8 conversion on Pt/Al_2O_3 catalyst for the selective catalytic reduction of NO by C_3H_8 under excess oxygen

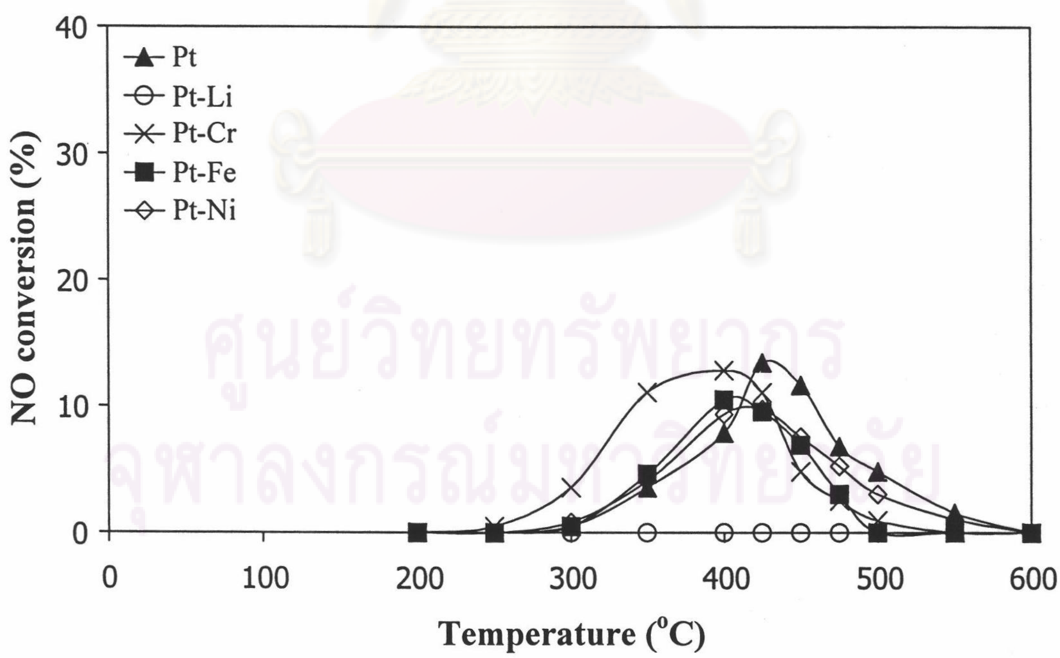

Figure 5.56 The effect of Li, Cr, Fe or Ni on NO conversion to N_2 on Pt/Al_2O_3 catalyst for the selective catalytic reduction of NO by C_3H_8 under excess oxygen

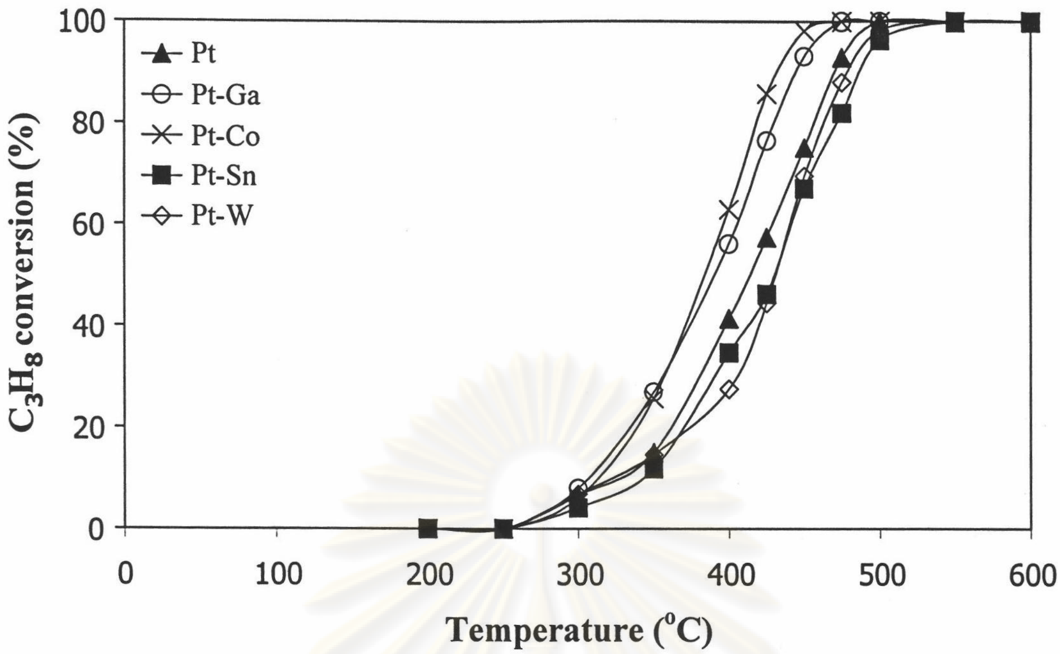

Figure 5.57 The effect of Ga, Co, Sn or W on C_3H_8 conversion on Pt/Al_2O_3 catalyst for the selective catalytic reduction of NO by C_3H_8 under excess oxygen

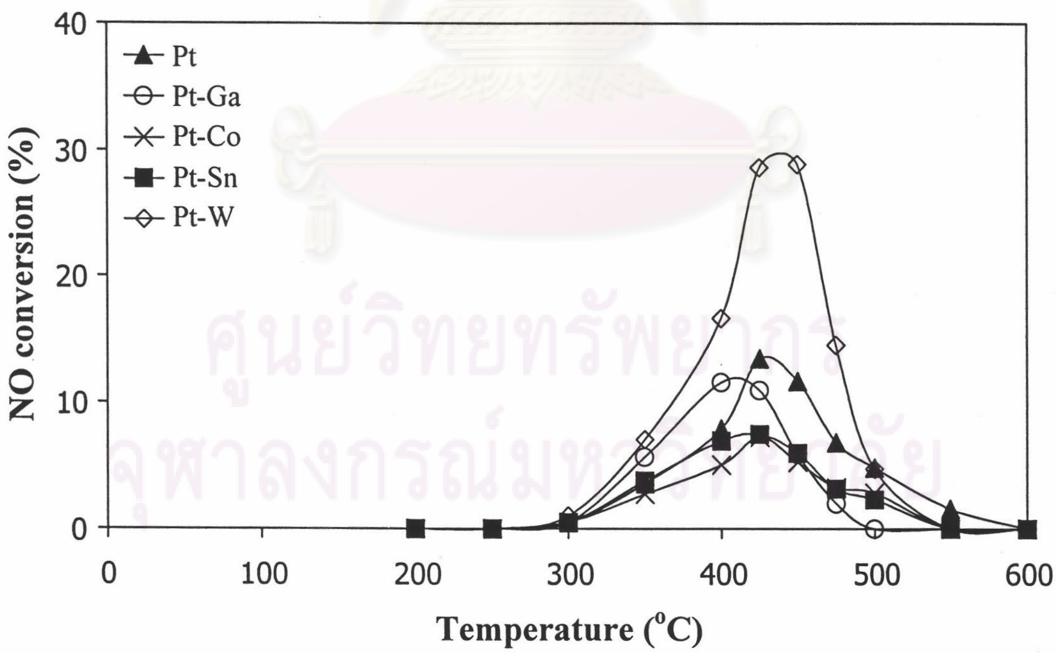

Figure 5.58 The effect of Ga, Co, Sn or W on NO conversion to N_2 on Pt/Al_2O_3 catalyst for the selective catalytic reduction of NO by C_3H_8 under excess oxygen

The addition of the second metal distinctly influences the C_3H_8 light-off temperature, the maximum NO conversion and the temperature of maximum NO conversion. The presence of Cr, Fe, Ni, Ga or Co on Pt/Al_2O_3 assists to lower the C_3H_8 light-off temperature. Unfortunately, the maximum NO conversions of these catalysts are relatively low compared to that of Pt/Al_2O_3. On the other hand, the C_3H_8 light-off temperature is shifted at higher temperature when Li, Sn and W are independently doped. Interestingly, the amount of N_2 on $Pt-W/Al_2O_3$ can be produced about two times more than that on Pt/Al_2O_3 at temperature of maximum NO conversion, although the C_3H_8 oxidation is slightly inhibited. It is noted that no production of N_2 over $Pt-Li/Al_2O_3$ catalyst is observed at all temperatures. Due to the decrease of acidity on Al_2O_3 after adding Li or vice versa doping W, it is believed that the formation of N_2 product involves the property of support, which is agreement in the open literature [159].

The difference of the catalytic activity behavior after the introduction of the second metal over Pt/Al_2O_3 catalyst does not affect the characteristic of surface species on modified Pt/Al_2O_3 catalysts, except $Pt-Li/Al_2O_3$, although their quantities is different. The carbon dioxide profiles obtained by the TPD step in an experimental set of three continuous steps for modified Pt/Al_2O_3 catalysts are shown in Figures 5.59 and 5.60. It is again remarked that the relatively small amount of nitrogen is detected and it is therefore neglected. Interestingly, the carbon dioxide can not be detected on only $Pt-Li/Al_2O_3$ catalyst, but a large amount of oxygen appears instead of carbon dioxide as shown in Figure 5.61.

From all results for the NO reduction with C_3H_8, it is concluded that an important step in the reaction mechanism for this reaction does not involve the complex surface species and therefore the investigation of surface species by temperature programmed technique in this work can not explain the reaction mechanism. Hence, the other characterizations are necessary to obtain the profound understanding in the catalytic activity behavior and next anticipate the reaction mechanism.

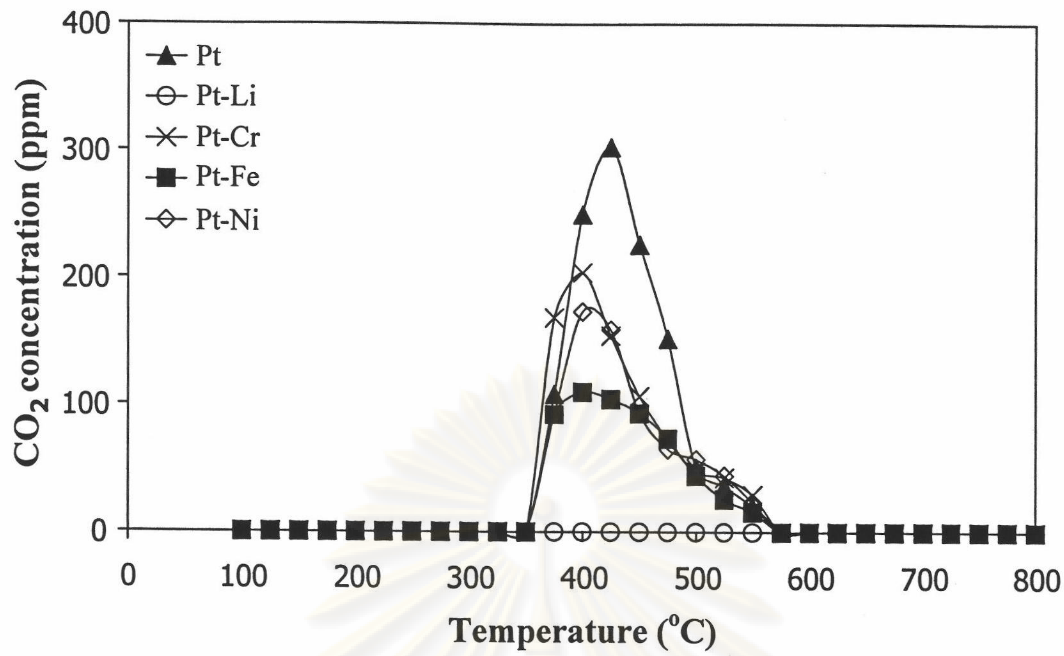

Figure 5.59 The carbon dioxide profiles of Pt, Pt-Li, Pt-Cr, Pt-Fe and Pt-Ni catalysts after dosing 1000 ppm C_3H_8 + 1000 ppm NO + 5% O_2 at 350°C for 2 h

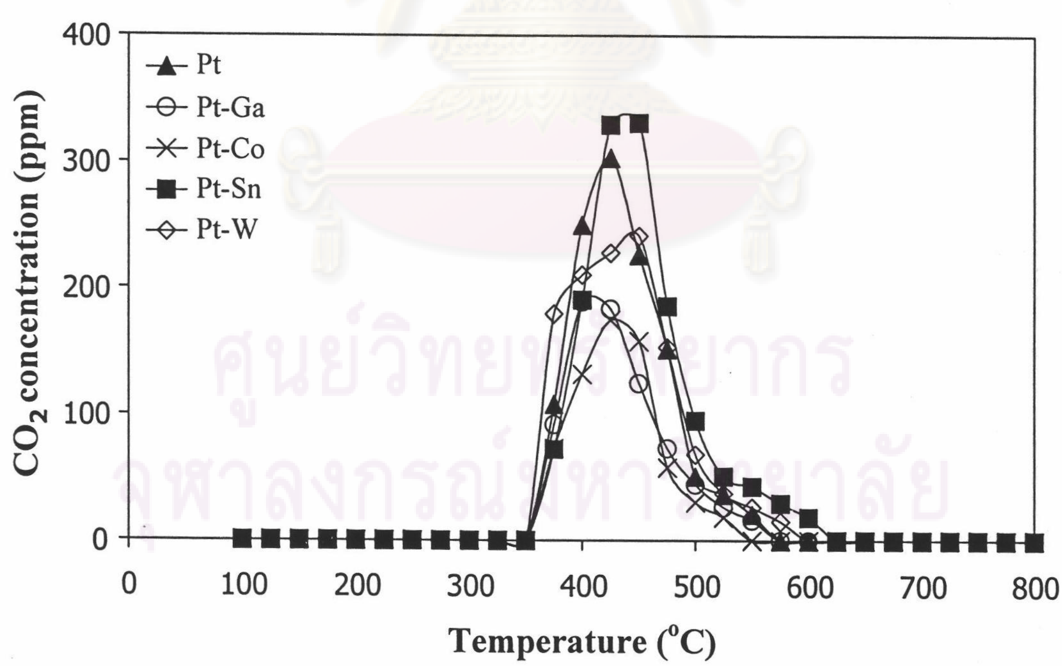

Figure 5.60 The carbon dioxide profiles of Pt, Pt-Ga, Pt-Co, Pt-Sn and Pt-W catalysts after dosing 1000 ppm C_3H_8 + 1000 ppm NO + 5% O_2 at 350°C for 2 h

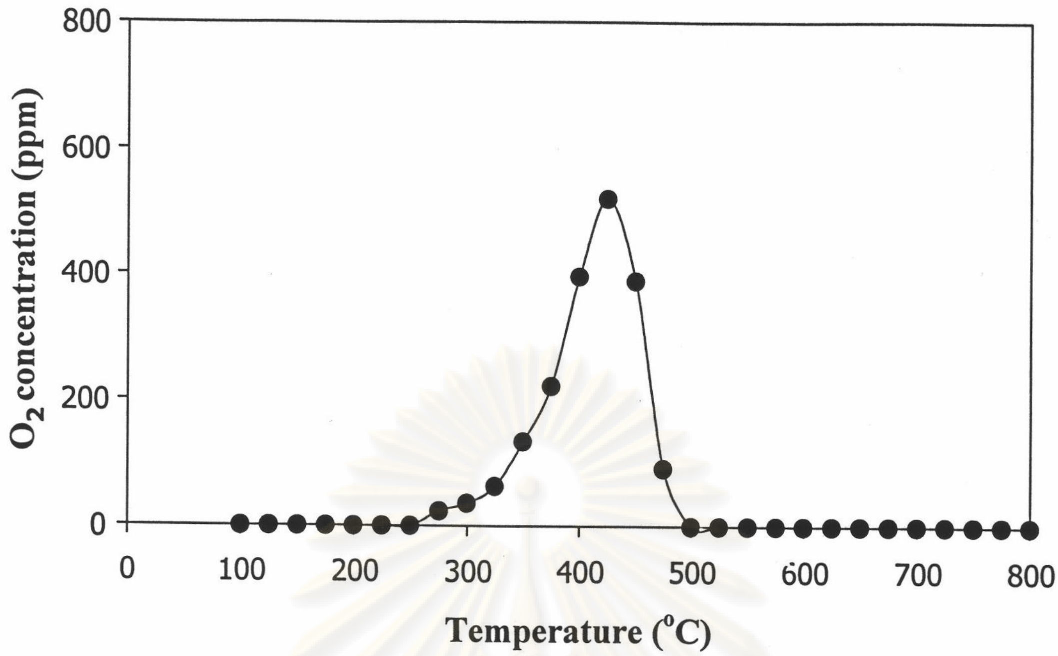

Figure 5.61 The oxygen profiles of Pt-Li catalyst after dosing 1000 ppm C_3H_8 + 1000 ppm NO + 5% O_2 at 350°C for 2 h